(NASA-CR-140329) INTEGRATED SOURCE AND CHANNEL ENCODED DIGITAL COMMUNICATION SYSTEM DESIGN STUDY Final Report (Axiomatix, Marina del Rey, Calif.) 65 p HC $4.25 CSCL 17B G3/32

N75-11136

Unclas
53[illegible]

[redacted]

# Axiomatix


Marina del Rey • California

# INTEGRATED SOURCE AND CHANNEL ENCODED DIGITAL COMMUNICATION SYSTEM DESIGN STUDY

FINAL REPORT

Contract No.: NAS 9-13467
Exhibit B

Prepared by

Gaylord K. Huth
Sergei Udalov

Axiomatix
13900 Panay Way, Suite 110M
Marina del Rey, California 90291

Prepared for

NASA Lyndon B. Johnson Space Center
Houston, Texas 77058

Axiomatix Report No. R7410-4
October 4, 1974

TABLE OF CONTENTS

## LIST OF TABLES

## LIST OF FIGURES

# I. INTRODUCTION

This study investigated the integration of a wideband communication system with a Ku-band rendezvous radar system. The goal of the study was to provide as much commonality between the two systems as possible. Thus, instead of making the communication system an add-on to an existing radar and only sharing the antenna and angle tracking system, the radar and the communication systems were investigated as an integrated system. A total system design was performed based on the radar and communication performance requirements presented in Section II.

The antenna design was retained with the only change being the requirement for dual polarization (linear for the radar system and circular for the communications system). Thus, the antenna is a 20-inch deployable dish Cassegrain with a four-horn monopulse feed system having a 35.4 dB gain and a $2.7^{\circ}$ bandwidth.

Commonality of transmitter and receiver components was stressed by considering the optimum relationship between TDRS (Tracking and Data Relay Satellite) communication frequencies and the radar operating frequency. One of the major contributing factors towards commonality was the consideration given to use of Interrupted CW (ICW) radar as opposed to high peak power, low duty cycle pulsed radar. Section III presents the summary of the ICW and compares its performance to the noncoherent pulse doppler

Section IV presents the integrated radar/communication system configuration. The overall system considerations such as polarization, transmitter tube characteristics and radar transmitter frequency selection are presented. An important aspect of the communication system design is the angular tracking of TDRS. Section IV presents analysis of angular tracking of TDRS using the communication signal directly rather than a special beacon. In the absence of the beacon, the detection of the condition of the communication antenna pointing at the TDRS (boresight detection) is performed by noncoherent integration and thresholding of the downlink communication signal which may be also a wideband spread-spectrum signal.

The baseline signal design for the communication system is presented in Section V. For the forward link, up to 1 Mbps of wideband data is quadrature PSK modulated with 72 kbps of operational data (8 kbps of encoded commands plus sync, and two 32 kbps voice channels). For the return link, up to 50 Mbps of wideband digital data is quadrature PSK modulated with up to 2 Mbps of digital data (which may be 192 kbps real time operational data). Alternately, on the return link, up to 2 Mbps digital data is quadrature PSK modulated with the 192 kbps operational data on a subcarrier and the subcarrier modulation is frequency modulated with either wideband analog data up to 4.2 MHz or up to 4 Mbps payload digital data.

While the baseline signal design uses quadrature PSK modulation, Section V also presents alternate modulation techniques that compare favorably with PSK modulation. Both binary and M-ary FSK are examined and the potential use of coding in conjunction with either of these modulation techniques is discussed. Use of both coherent and noncoherent detection schemes at the ground station is examined. These techniques are not baselined at this time due to the lack of experimental data needed to verify performance. This is an area of further study that needs to be performed, as discussed in Section VI. While the techniques for convolutional encoding/Viterbi decoding are presented in Section V, the need for further study of potential problem areas of operation at 50 Mbps such as the bit synchronization problem is described in Section VI. Other areas for further study outlined in Section VI include the need for additional angle acquisition and tracking analysis, detailed performance analysis of the rendezvous radar, and hardware implementation considerations. However, from the preliminary analysis summarized in this report, the coherent pulse doppler radar is the most promising for the integrated radar/communication system, both from the standpoint of performance and from the standpoint of weight, power, size, and cost.

# II. SPACE SHUTTLE Ku-BAND RADAR/COMMUNICATION SYSTEM

## 2.1 System Requirements

The requirements for the integrated radar/communication system are presented in this section to provide the basis for the system design that was performed.

The radar requirements are summarized in Table I. Note that, for a range rate of +100 ft/sec, the noncoherent pulse radar must detect the target at 12 nmi to allow the tracking loops to settle by the time the target reaches 10 nmi. The coherent pulse doppler radar does not require a long settling time; hence, the target can be detected at 11 nmi and still have the target tracking at 10 nmi.

The Shuttle communication system consists of the return link transmitter and forward link receiver. There is no requirement for signal turn-around coherency but crystal-controlled oscillators are recommended for both the transmitter exciter and receiver local oscillators to reduce drift and thus minimize the requirements for frequency search at the receiver. Use of a coherent synthesizer for the transmitter and receiver function is also consistent with the requirements of the ICW radar.

Table II presents the summary of the Shuttle communication requirements. Although not listed in the table, PN spectrum spreading may have to be applied to the forward data link to minimize spectral density falling upon the Earth. If used, such spreading may use PN sequence rates of up to approximately 14 Mbps.

## 2.2 System Block Diagram

The design philosophy for integrating the radar and the communication functions into a single system is illustrated by the basic block diagram of Figure 1. As shown in the figure, a single transmitter tube, a TWTA, is used to supply the antenna with either a high duty cycle pulsed radar signal or a CW communication signal. Such transmitter sharing is possible because of compatible output power level requirements for

the ICW doppler radar and the return communication link. Maximum commonality is also obtained in the receiver subunit which, with the exception of communication and radar processors, is shared by the two modes. A common crystal controlled synthesizer generates both the transmitter drive and the receiver local oscillator signals, thus providing for coherent operation of the pulse doppler radar and for reduction of frequency drifts in the communication system.

The sum channel output ($\Sigma$) of the monopulse generator provides the main received radar or communication signal which is amplified by one of the three parallel receiver channels.

Depending on the mode, the output of the sum channel receiver feeds either the communication or radar processor. The communication processor performs such functions as boresight detection of TDRS, PN code acquisition and tracking, doppler search and tracking, and data demodulation and decoding. The radar processor performs the initial target acquisition and subsequently tracks the range and range rate of the target.

The azimuth and elevation tracking error signals, $\Delta$AZ and $\Delta$EL, respectively, are also provided by the monopulse comparator. These error signals are amplified by the other two parallel receiver channels. The polarities and magnitudes of the angle errors are recovered by comparing them to the output of the sum channel receiver. The angle errors are then applied to the appropriate servos (not shown) to keep the antenna pointed, depending on the mode, at either the radar target or the TDRS.

In the radar mode, the receiver is isolated from the transmitter by the transmit/receive switches. The circulator provides additional isolation for the sum channel. In the communication mode, both the transmitter and the receiver are on continuously and thus their isolation is provided by proper front end filtering.

TABLE I

SHUTTLE RENDEZVOUS RADAR REQUIREMENTS

| | |
|---|---|
| **SEARCH REQUIREMENTS** | |
| • Angle Search Limits | $\pm 45^\circ$ about LOS - 2 axes |
| • Angle Rate | 4 mr/sec |
| • Detection of Acquisition Range | 10 nmi |
| • Probability of Detection | 0.99 |
| • False Alarm Rate | 1 per hour |
| • Range Rate | +100 ft/sec<br>- 50 ft/sec |
| • Acquisition (Reacquisition) Time | 60 (10) sec |
| **TRACKING REQUIREMENTS (3 Sigma Values)** | |
| • Angle | $\pm 10$ mr (random)<br>60 mr (bias) |
| • Angle Rate | 0.14 mr/sec (random)<br>0.14 mr/sec (bias) |
| • Range | $\pm 1\%$ of range (minimum of $\pm 2$ ft) |
| • Range Rate | $\pm 1$ ft/sec (random)<br>$\pm 1$ ft/sec (bias) |
| **ASSUMED TARGET CHARACTERISTICS** | |
| • Target Size | 1 $m^2$ |
| • Model | Swerling Case I |

TABLE II

SHUTTLE COMMUNICATION SYSTEM REQUIREMENTS

FORWARD LINK DATA HANDLING CAPACITY

Up to 1 Mbps wideband data and, simultaneously, 72 kbps operation data (two 32-kbps voice channels, plus 8 kbps encoded command sync)

| | |
|---|---|
| Bit error probability | $10^{-6}$ |
| Coding | V = 3, K = 7 |

RETURN LINK DATA HANDLING CAPACITY

Mode 1: Simultaneous transmission of the following:

a) Up to 2 Mbps digital data which may include

real time 192 kbps operational data

or playback of recorded data from maintenance/loop recorders

or playback from experimental PCM recorder

or real time experimental data

b) Up to 50 Mbps wideband digital data (real time or playback)

| | |
|---|---|
| Bit error probability | $10^{-6}$ |
| Coding | V = 2, K = 7 |

Mode 2: Simultaneous transmission of the following:

a) Wideband analog up to 4.2 MHz (television or payload analog data) or up to 4 Mbps payload digital data

b) Up to 2 Mbps digital data (playback of recorded operational data from the maintenance/loop recorders)

or playback from experimental PCM recorder

or real time payload data

| | |
|---|---|
| FM output SNR (rms/rms) | 26 dB |
| Bit error probability | $10^{-6}$ |

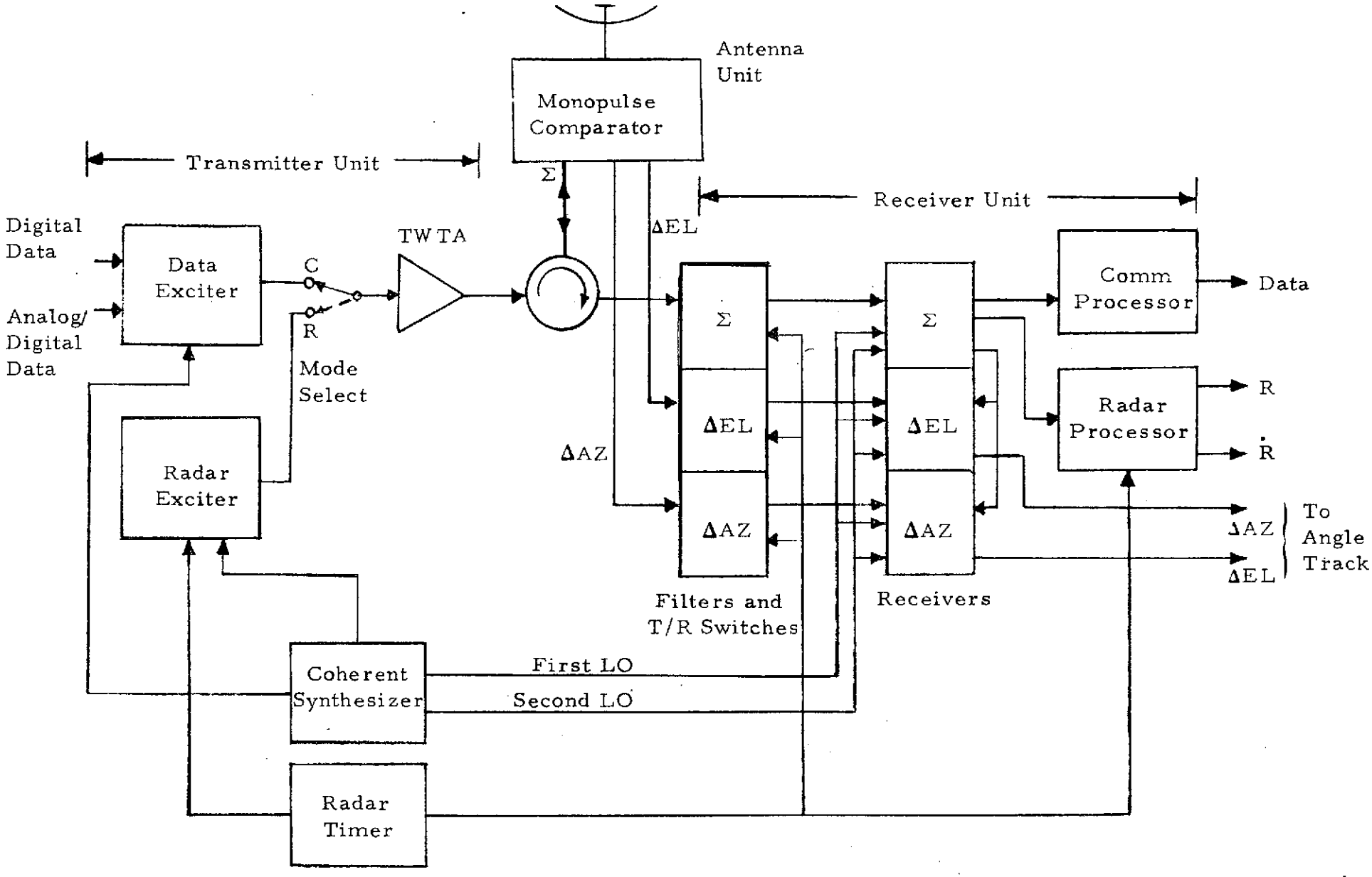


Figure 1. Basic Block Diagram for an Integrated Radar/Communication System

## III. SUMMARY OF THE RADAR SYSTEM

The optimization of a center line Ku-band coherent pulsed doppler radar has been performed in its search mode [1]. The configuration was chosen to maximize the number of components that are common to both the radar and communication operations.

It is shown that the coherent pulsed doppler radar can operate within all search mode specifications with a peak transmitter power of less than 20 watts, providing at least a 3 dB design margin with respect to the 40 watts average power required for the communications.

The radar is designed so that the radar frequency is close to the communications receive frequency. It is anticipated that this will provide no problem of interference with other users of the TDRS.

A detailed analysis is presented of the noncoherent pulsed radar to provide a clear comparison with the coherent radar. It is shown that the power requirements of the coherent radar are uniformly smaller than those of the noncoherent radar. The difference in requirements is quite small in many of the cases considered.

Figure 2 is a block diagram of a center line coherent pulsed doppler radar (ICW) operating in the search mode. In this implementation, the design is carried out to maximize the number of components which can be used both in the radar and communication subsystems of the shuttle Ku-band radar/communication system. In this design, the radar center frequency is located close to the communication receive frequency. Inspection of Figure 2 shows the components that are used in both the radar and communication Ku-band operation. The communication system operates through the TDRS and cannot operate simultaneously with the rendezvous radar. In determining the performance of this system, several system parameters are varied: number of scans, number of RF frequencies used in frequency diversity, and choice of polarization. Several optimizations have also been carried out.

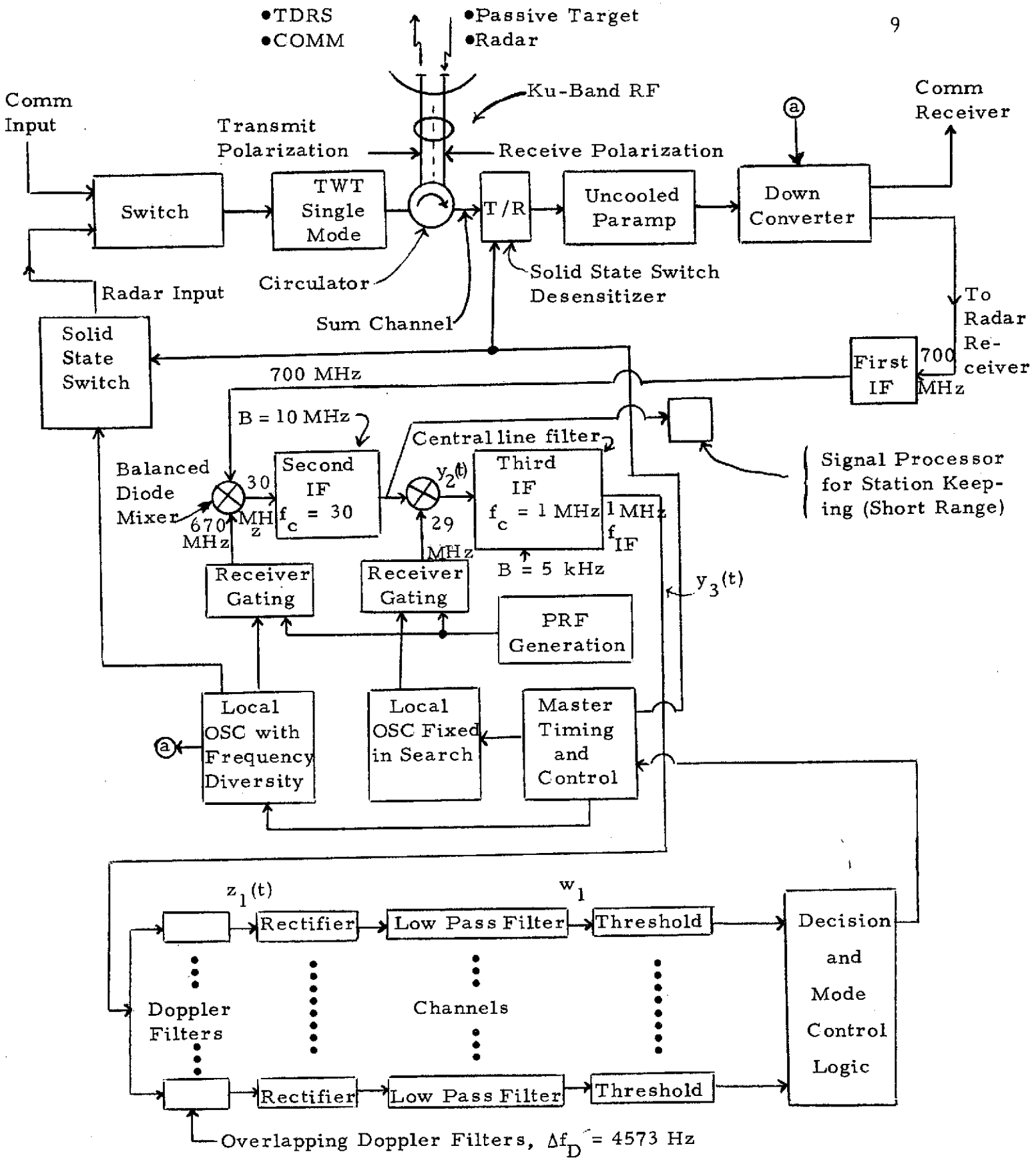


Figure 2. Center Line Pulsed Doppler Radar Receiver in Search Mode Where Radar Frequency is Close to the Comm Receive Frequency.

The communication receiver employs an uncooled paramp. The radar receiver in this implementation uses the same paramp, which has a noise figure of about 3 dB, as compared to the balanced diode mixer (see Figure 2) of F ≈ 8 dB. The balanced diode mixer is not as sensitive to large inputs as the uncooled paramp. The T/R switch may have to be used as an attenuator at shorter ranges, or the transmitter power reduced to protect the targets being tracked.

The paramp shown in Figure 2 is the only such device in this configuration of the integrated radar/communication system. The paramp is located in the sum channel of the monopulse horn output. It is anticipated that a paramp receiver amplifier will not be required in the two difference channels, because of the long time constant in the angle tracking loops, thereby providing sufficient smoothing to obtain sufficiently high signal-to-noise ratio. The sum and difference channels will then have unequal gains. These can be monitored and taken into account in the subsequent signal processing.

## 3.1 Considerations for the Integrated Components

A. Uncooled Paramp - Ku-Band

1) A noise figure of 2-3 dB at 15 GHz as compared to a noise figure of 8 dB for the balanced diode mixer at 15 GHz (ref. Skolnick [2, Ch. 5]).

2) The uncooled paramp (and single mode TWT transmitter amplifier) are essentially not off-the-shelf items that are space qualified. The technology is there, however, which for these components in this frequency band is the best that can be expected at this point in time.

3) The bandwidth of an uncooled paramp in the Ku-band is approximately 500 MHz. This is more than sufficient bandwidth to be used as the low noise front end RF amplifier for both radar and communications, provided the radar frequency is close to or equal to the communications receive frequency. This is the case whether or not frequency

diversity is employed by the radar. This places the radar frequency in the TDRS band. This should not produce any problems since the radar and Ku-band communications to the TDRS can never be operating simultaneously.

4) When the noise figure is as low as 2-3 dB for the RF amplifier of the receiver, it may be necessary to take into account the noise temperature of the antenna. When the balanced diode mixer is the first RF component, then $F \approx 8$ dB, and $T_s \approx 1540^{\circ}K$, so that the antenna temperature can be neglected. For the uncooled paramp with $F \approx 3$ dB, then $T_{paramp} \approx 290^{\circ}K$, and the antenna temperature could be significant. To date, we are not aware of an approximate noise temperature being specified for the antenna.

B. Single-Mode TWT Transmitter Amplifier

1) Single cathode, thereby employing a simpler power supply and support equipment and probably less weight overall.

2) With a single cathode, the radar is peak power limited and the communications is average power limited.

3) By comparison, the dual-mode TWT could be considered with two cathodes, one for radar and one for communications. Both systems would then be average power limited and the radar could transmit a much higher peak power. This implementation requires a dual power supply and more support equipment.

C. Frequency Diversity

In most cases, under the assumption of a Swerling I target model, it will be possible to maintain performance requirements without employing frequency diversity in the search mode of radar operation. In view of the following comments, however, some frequency diversity is going to be required.

1) The glint effects at short ranges will be sufficient so that angle tracking will not be able to be maintained within specifications without frequency diversity. Frequency diversity is very effective in reducing those glint effects.

2) The class of targets that are anticipated remains unknown. To offset the deep fades in RCS of many targets at a fixed frequency as a function of aspect angle, frequency diversity should be employed.

3) There are guard spaces in the TDRS spectrum which could be used by the Ku-band radar with frequency diversity. Whether they are used, or if the radar frequencies are placed on the edge of the TDRS band, the performance will be essentially unchanged so long as the bandwidth of the TDRS (communications) spectrum and that of the radar remain within the bandwidth of the paramp. Otherwise, separate RF receiver amplifiers will have to be employed, thereby reducing the commonality of the integrated system.

4) The width of the frequency spacing must be considered. This is discussed in references 3 and 4. In summary, for a two point target with an orientation as shown in Figure 3, if the shift in frequencies of two adjacent frequencies in a frequency diversity radar is such that at one frequency the returns add, and at the other they cancel, then

$$\Delta f_c = \frac{c}{4D \cos \alpha} \tag{1}$$

In (1), c is the speed of light and D and $\alpha$ are as defined in Figure 3.

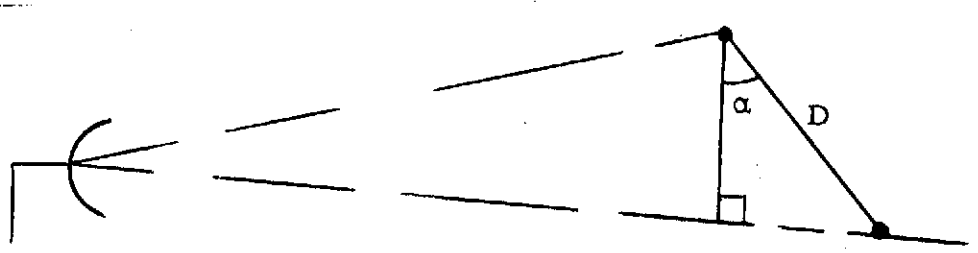


Figure 3. Two Point Target Orientation

A few examples of this are:

| $D \cos \alpha$ (meters) | $\Delta f$ (MHz) |
|---|---|
| 1 | 75 |
| 10 | 7.5 |
| 100 | 0.75 |

The guard spaces in the TDRS spectrum are separated by approximately 70 MHz. Therefore, if $D \cos \alpha$ is as small as 1 meter, frequency diversity with a $\Delta f_c$ of 70 MHz would remove the nulls in the RCS.

5) A typical target for the Shuttle is the Agena, although a wide variety of target sizes and shapes is anticipated.

6) The RCS of $\bar{\sigma} = 1\ m^2$ assumes a linear polarization.

7) Scintillation occurs slowly with one frequency. This may cause problems, but is overcome by more than one RF frequency.

D. Oscillator Stability

The choice of bandwidth of the doppler filters must take into account the short term stabilities of the oscillators that are to be used. References 5, 6, and 7 discuss oscillator stability, wherein it is pointed out that, in the Ku-band, oscillators exist with a frequency spread of:

| RMS Percent bandwidth |
|---|
| 1 part in $10^{10}$ in 0.001 sec |
| 1 part in $10^{12}$ in 1 sec |

This is negligibly small with respect to the doppler frequency shifts that are anticipated and is therefore not taken into account henceforth.

E. Polarization

1) For most radars, linear polarization is used because it is easier to implement and has more desirable target RCS characteristics.

2) Satellites and deep space communication systems mostly use circular polarization in order to overcome the effects of the Faraday rotation in the terrestrial ionosphere. TDRS is no exception, as it

transmits and receives RCP. It actually has a slightly elliptical shaped polarization.

3) A basic problem in the choice of a receiver polarization for the radar is that there will always be an orthogonal polarization to which it is blind. A radar could independently receive two polarizations, such as horizontal and vertical simultaneously, in order to receive all the echo energy. These could not be added coherently, however.

4) In general, measurements show that with linear polarization, the radar skin tracking echo signal is dominantly the same polarization as the transmitter polarization, and the cross-polarized component caused by depolarization due to the complex shaped target is typically 7-20 dB lower [2,3], depending on the aspect angle.

5) With circular polarization, for any one sense of transmitter polarization, the echo signal is typically equally divided between RCP and LCP. The opposite sense dominates somewhat for typical aircraft-type targets [2,3].

6) The total echo signal returned from a target is very dependent on its orientation, i.e., a dipole.

7) If the Ku-band communications receiver is linearly polarized, it would nominally suffer a 3 dB polarization loss, since the TDRS is circularly polarized. Since the TDRS is elliptically polarized, the worst case loss is 4.4 dB, 3 dB because it is circular and an additional 1.4 dB when on the smaller axis of the elliptical polarization.

We conclude the communication system must therefore use circular polarization since the communication system does not have the safety margin to withstand an additional 4 dB loss. The communication polarization loss with a circularly polarized horn is 0.5 dB, which accounts for the difference between the elliptical wave and circularly polarized horn.

8) The performance computations in [1] are carried out for both a linearly and circularly polarized horn. With linear polarization, the polarization loss is assumed negligible. With the circularly polarized

horn, the polarization loss is set at 4 dB which is considered a representative worst case.

9) Independent of which polarization is employed, there exist targets and target orientations where the polarization loss is infinite. On the average, however, linear polarization is certainly the more satisfactory choice.

10) With linear polarization for the radar and circular polarization for the communications, then a dual feed is required which requires more hardware. There then is an insertion loss due to the dual feed as well as a drop in antenna gain because both feeds cannot be exactly at the focal point of the antenna. The drop in antenna gain is expected to not be more than 1 dB.

11) Autonetics is developing a dual polarization single feed horn system with both linear and circular polarization capability.* If such a horn can be space-qualified, and if the polarization switching is electromagnetic (mechanical polarization switching runs the risk of getting stuck in one mode or in between), then a linear polarization for the radar is certainly the recommended choice. Such a dual horn must also have the monopulse capability. There are other dual horn developments in progress. The antenna and insertion losses are expected to be similar to those quoted above.

12) The RCS of an object in general depends on: frequency of incident radiation; polarization of the transmitter; polarization of the receiver; target orientation; and material of the target.

## 3.2 Comparison of Performance for the Coherent and Noncoherent Radars

The Ku-band coherent pulse doppler radar (ICW) has been analyzed [8] and subsequently optimized [1]. Three different criteria were considered

*Reference B. McQuillan at Rockwell.

in Appendix A of Reference 1 to choose the optimal antenna scan overlap. Each of these criteria have reasons for which it can be considered conceptually unsatisfactory. A more satisfactory criterion is employed in Reference 9 which tends to make the energy return reasonably uniform across the non-overlapping position of the antenna pattern. With this new criterion, the optimal choice of scan overlap is $\Delta_s = 0.25$.

As a result of the optimization of the coherent pulse doppler radar [1], the required average power and peak power are tabulated in Table III for K = 1, 2, 3 scans, and 1, 2, 3, and 6 RF frequencies. Reference 10 has performance curves for six pulses, and not five. It is anticipated that the difference between six and five is not very great, so that the trade-off that is being shown is clearly established.

Let us assume that the average power requirement of the communications system is approximately 40 watts, and that the peak power of the radar (in the coherent system) is not to exceed the communications requirement. It then becomes clear which cases qualify by inspection of Table III. For linear polarization, the choices are greater. It is clear that circular polarization cannot be used unless at least three frequencies of diversity are used, and five frequencies will not provide a substantial safety margin. With circular polarization and five frequencies of diversity, either one scan or two scans will provide a satisfactory design. With linear polarization, it would be possible to eliminate frequency diversity in the search mode. Because of the necessity of frequency diversity for angle tracking, frequency diversity with three frequencies is proposed. This provides over 3 dB of safety margin, regardless of the number of scans chosen.

In some of the cases, the required peak power as a function of the number of scans has a minimum value at K = 2 scans.

The optimal choice of number of scans is dependent on the choice of frequency diversity and vice versa. The optimal choice of the combination is case 4, namely, one scan and five frequencies of diversity.

TABLE III

POWER REQUIREMENTS FOR COHERENT PULSED DOPPLER CENTER LINE RADAR

| Case | Number of Scans | Number of RF Freq. | Polarization | R dB | $\bar{R}_p$ dB | Freq Dwell Time $\tau_t$ msec | $\tau_t$ dB | $P_p$ dB | $P_p$ Watts | $P_{avg}$ Watts |
|---|---|---|---|---|---|---|---|---|---|---|
| 1 | 1 | 1 | L | 0 | 36.5 | 110 | - 9.59 | 24.52 | 283.1 | 177 |
| 2 | 1 | 2 | L | 0 | 24 | 55 | -12.60 | 15.03 | 31.8 | 19.9 |
| 3 | 1 | 3 | L | 0 | 19.7 | 37 | -14.32 | 12.45 | 17.6 | 11.0 |
| 4* | 1 | 5(6) | L | 0 | 14.5 | 22 | -16.58 | 9.51 | 8.9 | 5.6 |
| 5 | 2 | 1 | L | 0 | 24 | 55 | -12.60 | 15.03 | 31.8 | 19.9 |
| 6 | 2 | 2 | L | 0 | 18.5 | 27.5 | -15.61 | 12.54 | 17.9 | 11.2 |
| 7 | 2 | 3 | L | 0 | 15.7 | 18.3 | -17.38 | 11.51 | 14.2 | 8.8 |
| 8* | 2 | 5(6) | L | 0 | 12 | 11 | -19.59 | 10.02 | 10 | 6.3 |
| 9 | 3 | 1 | L | 0 | 21.3 | 37 | -14.32 | 14.05 | 25.4 | 15.9 |
| 10 | 3 | 2 | L | 0 | 16.3 | 19 | -17.21 | 11.94 | 15.6 | 9.8 |
| 11 | 3 | 3 | L | 0 | 14 | 12 | -19.21 | 11.64 | 14.6 | 9.1 |
| 12* | 3 | 5(6) | L | 0 | 10.7 | 7.4 | -21.31 | 10.44 | 11.1 | 6.9 |
| 13 | 1 | 1 | C | 4 | 36.5 | 110 | - 9.59 | 28.52 | 711. | 445. |
| 14 | 1 | 2 | C | 4 | 24 | 55 | -12.60 | 19.03 | 80. | 50. |
| 15 | 1 | 3 | C | 4 | 19.7 | 37 | -14.32 | 16.45 | 44.2 | 27.6 |
| 16* | 1 | 5(6) | C | 4 | 14.5 | 22 | -16.58 | 13.51 | 22.4 | 14.0 |
| 17 | 2 | 1 | C | 4 | 24 | 55 | -12.60 | 19.03 | 80. | 50.0 |
| 18 | 2 | 2 | C | 4 | 18.5 | 27.5 | -15.61 | 16.54 | 45.1 | 28.2 |
| 19 | 2 | 3 | C | 4 | 15.7 | 18.3 | -17.38 | 15.51 | 35.6 | 22.2 |
| 20* | 2 | 5(6) | C | 4 | 12 | 11 | -19.59 | 14.02 | 25.2 | 15.8 |
| 21 | 3 | 1 | C | 4 | 21.3 | 37 | -14.32 | 18.05 | 64.8 | 39.9 |
| 22 | 3 | 2 | C | 4 | 16.3 | 19 | -17.21 | 15.94 | 39.3 | 24.6 |
| 23 | 3 | 3 | C | 4 | 14 | 12 | -19.21 | 15.64 | 36.6 | 22.9 |
| 24* | 3 | 5(6) | C | 4 | 10.7 | 7.4 | -21.31 | 14.44 | 27.8 | 17.4 |

*Calculation based on six individual RF frequencies.

In order to obtain some system simplicity, if the number of frequencies of diversity is reduced to three, then the optimal choice is two scans.

One can see, however, that there is not an extensive variation in the peak power requirement over all of the cases listed above, and any of these would make a satisfactory design.

If a low PRF is used so that eclipsing loss is essentially eliminated in the range of 10-15 nmi, then a safety margin of over 7 dB can be gained. When this is the case, there is the probability of detecting the incorrect line in the coherent spectrum. If the transition from detection to tracking can be smoothly carried out, however, then that may be the most satisfactory implementation of the coherent radar.

To compare the performance of a noncoherent Ku-band pulsed radar in the search mode of operation with the performance of the coherent pulsed doppler radar, as many of the system parameters as possible are kept the same so as to provide a satisfactory comparison. The analysis of the noncoherent pulsed radar is presented in Reference 1. Frequency diversity and a fluctuating Swerling I target were considered, as for the coherent pulsed doppler radar. When considering frequency diversity with a pulsed radar, the question arises as to the method of obtaining the necessary frequency agility. There are at least three methods:

1) Mechanical Spin Tuning. This is old technology and much too slow for the kind of frequency diversity required.

2) Voltage-Tunable Magnetron. The bandwidth is attainable by this method but this method is power limited as a pulsed radar. It is more commonly used in CW radars.

3) Injection Locking. This method consists of priming the magnetron at a given frequency, then pulsing it. This will provide the necessary frequency diversity, but it is very inefficient.

These methods are discussed in Skolnick [2, Ch. 7]. The present-day methods of attaining a 3 percent bandwidth frequency diversity for a

pulsed radar are presently being investigated. There is the additional consideration of insuring that the paramp has adequate protection from the magnetron both in the transmit and receive modes of operation.

In Table IV, the parameters of the pulse radar are listed. The 3 dB IF bandwidth is chosen as the reciprocal of the pulse width.

TABLE IV

PULSE RADAR PARAMETERS

| | |
|---|---|
| Pulse width | 0.4 $\mu$sec |
| IF bandwidth | 2.5 MHz |
| PRF | 2500/sec |
| Pulse repetition time | 400 $\mu$sec |
| Transmitter duty factor | 0.001 |

The performance of the noncoherent pulsed radar is presented in Table V, where the cases are numbered in the same way as in Table III for the coherent pulse doppler radar. For a given case number, the number of scans, the number of RF frequencies of diversity, the polarization, and the frequency dwell time are the same in both Table III and Table V.

Comparison of Tables III and V shows that the average power requirement for the coherent radar is uniformly better than for the noncoherent radar, but not by a great margin for the cases of most interest. The coherent system has a larger number of components integrated with the communications system than does the noncoherent. The magnetron transmitter must also have its necessary accessories such as power supply and cooling equipment, which also would not be integrated with the communications system. It is therefore anticipated that the total weight of the radar/communications system will be less with the coherent radar.

TABLE V

POWER REQUIREMENTS FOR NONCOHERENT PULSED RADAR

| Case | N Number of Pulses/ Frequency | Net Frequency Diversity Gain $G_D$, dB | Fluctuating Target Loss $L_F$, dB | $\lambda$ | $\lambda$ dB | Polarization p dB | $P_p$ dB | $P_p$ kw | $P_{avg}$ w |
|---|---|---|---|---|---|---|---|---|---|
| 1 | 275 | 0 | 17.8 | 1.0 | 0 | 0 | 53.44 | 220 | 220 |
| 2 | 137 | 9.5 | 17.8 | 1.0 | 0 | 0 | 43.94 | 24.7 | 24.7 |
| 3 | 92 | 12. | 17.8 | 1.0 | 0 | 0 | 41.44 | 13.9 | 13.9 |
| 4 | 55 | 14.2 | 17.8 | 1.0 | 0 | 0 | 39.24 | 8.4 | 8.4 |
| 5 | 137 | 0 | 8.5 | 1.18 | 0.72 | 0 | 44.86 | 30.6 | 30.6 |
| 6 | 68 | 2.3 | 8.5 | 1.18 | 0.72 | 0 | 42.56 | 18.0 | 18.0 |
| 7 | 45 | 3.5 | 8.5 | 1.18 | 0.72 | 0 | 41.36 | 13.7 | 13.7 |
| 8 | 27 | 4.2 | 8.5 | 1.18 | 0.72 | 0 | 40.7 | 11.6 | 11.6 |
| 9 | 92 | 0 | 5.2 | 1.29 | 1.11 | 0 | 41.95 | 15.7 | 15.7 |
| 10 | 47 | 2 | 5.2 | 1.29 | 1.11 | 0 | 39.95 | 9.9 | 9.9 |
| 11 | 30 | 2.5 | 5.2 | 1.29 | 1.11 | 0 | 39.45 | 8.8 | 8.8 |
| 12 | 18 | 2.8 | 5.2 | 1.29 | 1.11 | 0 | 39.15 | 8.2 | 8.2 |
| 13 | 275 | 0 | 17.8 | 1.0 | 0 | 4 | 57.44 | 554. | 554. |
| 14 | 137 | 9.5 | 17.8 | 1.0 | 0 | 4 | 47.94 | 62.2 | 62.2 |
| 15 | 92 | 12.0 | 17.8 | 1.0 | 0 | 4 | 45.44 | 35 | 35 |
| 16 | 55 | 14.2 | 17.8 | 1.0 | 0 | 4 | 43.24 | 21.1 | 21.1 |
| 17 | 137 | 0 | 8.5 | 1.18 | 0.72 | 4 | 48.86 | 76.9 | 76.9 |
| 18 | 68 | 2.3 | 8.5 | 1.18 | 0.72 | 4 | 46.56 | 45.3 | 45.3 |
| 19 | 45 | 3.5 | 8.5 | 1.18 | 0.72 | 4 | 45.36 | 34.4 | 34.4 |
| 20 | 27 | 4.2 | 8.5 | 1.18 | 0.72 | 4 | 44.7 | 29.5 | 29.5 |
| 21 | 92 | 0 | 5.2 | 1.29 | 1.11 | 4 | 45.95 | 39.4 | 39.4 |
| 22 | 47 | 2 | 5.2 | 1.29 | 1.11 | 4 | 43.95 | 24.8 | 24.8 |
| 23 | 30 | 2.5 | 5.2 | 1.29 | 1.11 | 4 | 43.45 | 22.1 | 22.1 |
| 24 | 18 | 2.8 | 5.2 | 1.29 | 1.11 | 4 | 43.15 | 20.6 | 20.6 |

For all of these reasons, the coherent radar appears the more satisfactory choice and is therefore our recommendation. Several cases have been shown to provide satisfactory operation with a safety margin of near 6 dB with respect to an average power requirement of 40 watts for communications.

An additional consideration in comparing the coherent and noncoherent radars is the tracking of range rate. In a coherent radar, the range rate of the target is tracked directly since the initial detection is based upon the doppler frequency. A doppler tracking loop is placed into operation upon target detection. The settling time of a doppler tracking loop is negligible with respect to changes in range (milliseconds).

In the noncoherent radar, range rate must be determined indirectly through filtering and differentiation of range measurements. A key difficulty in the noncoherent system is the initial settling time for the estimator and additional settling time after an acceleration.

An initial analysis of range rate tracking in the noncoherent pulsed radar is presented in Reference 11. However, a more refined analysis is necessary and this is an area that needs further study. It should be pointed out that the coherent system will outperform the noncoherent system from the range rate estimation viewpoint, both in settling time and estimate accuracy.

## 3.3 Short Range Considerations

In this section, a sequence of comments are presented concerning the operation of the radar at short range in stationkeeping.

1. To protect the paramp, the T/R switch may have to be partially engaged at short ranges. In addition, in order to protect the targets, the TWT will need to be reduced in power or bypassed. The latter will, in all likelihood, be the most satisfactory approach.

2. The scintillation and glint at short ranges will be very large. Therefore, frequency diversity will virtually be a requirement in order to substantially reduce these effects at short ranges.

3. At short ranges, stationkeeping may be more effectively performed via doppler frequency instead of range. One of the reasons for this is the ratio of target size to range becomes so large that the definition of range and the capacity of measuring range comes into doubt. If this is the case, a coherent radar with doppler tracking capability will be the more acceptable approach.

4. Approximately, the far field of an antenna starts at $R_{FF} \approx 2d^2/\lambda$ where d is the diameter of the antenna. For a 20" dish, $R_{FF} \approx 25.8$ m = 85 feet. Stationkeeping at 100 feet is therefore close to the edge of the far field of the antenna.

# IV. SUMMARY OF INTEGRATED RADAR/COMMUNICATION SYSTEM CONFIGURATIONS

In the preceding section, the radar mode of the integrated radar/communication system was described in detail. We will consider now, in more detail, the various aspects of integrating the radar and communication functions into one compatible configuration. Additional aspects of communication system performance will also be considered.

## 4.1 Overall Considerations

### 4.1.1 Polarization

The importance of using optimum polarization for the radar and communication modes has been discussed in paragraph 3.1. It was pointed out that, for radar, the linear polarization was the best choice and that, for compatibility with TDRS antennas, circular polarization is optimum. Because we are limited to a single antenna, polarization selection must be accomplished either within the feed or subreflector structure. For example, an antenna with a subreflector which, when rotated, can change the antenna's polarization from circular to linear and vice versa will be considered. Dual polarization, single feed horn systems, with both circular and linear polarization capabilities are also being developed. Thus, there is a good possibility that an off-the-shelf antenna may be available. We will therefore assume that, for the communications links, both forward and return, the polarization loss will be limited to about 0.5 dB.

### 4.1.2 Radar Frequency Selection

The operating frequencies of the Orbiter's transmitter and receiver are determined by the characteristics of the TDRS satellite. Selection of the radar frequency is subject to system integration considerations.

Initially, it had been assumed that the Orbiter receive (forward link) frequency will be 14.90 GHz and that there will be a beacon at 14.94 GHz. Consequently, a radar frequency of about 15.3 GHz was contemplated.

However, according to Reference 13, the Orbiter receive and transmit frequencies, as well as bandwidth associated with these frequencies, are as follows:

| | | Frequency | Bandwidth |
|---|---|---|---|
| $T_x$: | Ku-Band User Forward Link (TDRS to Orbiter) | 13.775 GHz | 50 MHz |
| $R_x$: | Ku-Band Return Link (Orbiter to TDRS) | 15.0085 GHz | 225 MHz |

Also, as mentioned previously, there may not be a separate beacon channel and thus tracking of the received signals, both at the Orbiter and at the TDRS, may have to be performed directly on the communication signals.

The approximate 1.5 GHz separation between 13.775 GHz communication receive and 15.3 GHz radar frequency precludes the use of a common low noise parametric amplifier for the radar sum channel because typical maximum state-of-the-art bandwidths for X and Ku-band paramps are about 0.5 GHz. A parametric amplifier in the radar channel, however, is desirable from the standpoint of improving radar system performance. Furthermore, the communication frequencies listed above make the use of 15.3 GHz for radar frequency somewhat questionable, particularly from the standpoint of isolating the CW communication transmitter from the receive channels which, for the sake of commonality, should be close in frequency for both the communication and radar modes.

Filter requirements for the receive channels also influence the selection of radar operating frequency. Specifically, if the radar frequency is above the communication transmit frequency, diplexers with selectable outputs must be placed in all three receive channels, i.e., $\Sigma$, $\Delta$AZ, and $\Delta$EL. The purpose of such diplexers would be to suppress the CW communication transmit signal but to pass either the radar or communication receive signals to the inputs of the three receivers.

An alternate approach is to use a band-reject filter at the communication transmit frequency. The selectivity characteristic of such a filter must be such that it provides very little attenuation to the adjoining radar

15.3 GHz signal. Whether such a filter can be obtained is a matter for further investigation.

Consequently, the baseline system presently under consideration by Axiomatix is based on the assumption that the radar frequency can be made either equal or close to the communication receive frequency. Such placement will permit the use of the low noise parametric amplifier for the radar as well as for the communication channels and will reduce the receiver channel filtering requirements to only a single bandpass filter in each receive channel.

### 4.1.3 Transmitter Tube Characteristics

The proposed integrated communication/radar system requires a 40-watt traveling wave tube (TWT) with the capability of operating both in a CW and a pulsed mode. Two of the major TWT vendors indicated that such a TWT can be produced (with some additional engineering development) by incorporating a modulating grid into a modified version of a 200-watt, 12 GHz high efficiency tube. The grid is required to modulate the electron beam at pulse repetition rates up to 150 kHz for the radar mode. Since most helix tubes are rated up to 40 watts and cannot afford the power degradation caused by the electron beam blockage by the grid, the coupled cavity TWT which has higher available output power levels is recommended [12]. Some typical specifications for a coupled cavity TWT which satisfies the integrated communication radar system are listed in Table VI.

## 4.2 Detailed Block Diagram

### 4.2.1 Functional Description

The overall block diagram of the Integrated Ku-Band Radar/Communication System is shown in Figure 4. Note that most of the receiver local oscillator and transmitter excitation frequencies are derived by multiplication from a common crystal controlled frequency synthesizer. The signal coherency provided by such an approach is of particular

TABLE VI

COUPLED CAVITY TWT PARAMETERS FOR THE SHUTTLE INTEGRATED COMMUNICATION/RADAR SYSTEM

| | |
|---|---|
| Power Output | 40 watts minimum |
| Modulation | Gridded |
| Grid Voltage | ±50 volts with respect to cathode voltage |
| Cathode Voltage | -8 kilovolts |
| Cathode Current | 31 mA |
| Center Frequency Range | 13 to 15 GHz |
| RF Bandwidth | 500 MHz |
| Gain | 40 to 50 dB |
| Collector | 4-stage depressed electrodes, 0 to -7 kilovolts |
| Overall Efficiency | 40% |

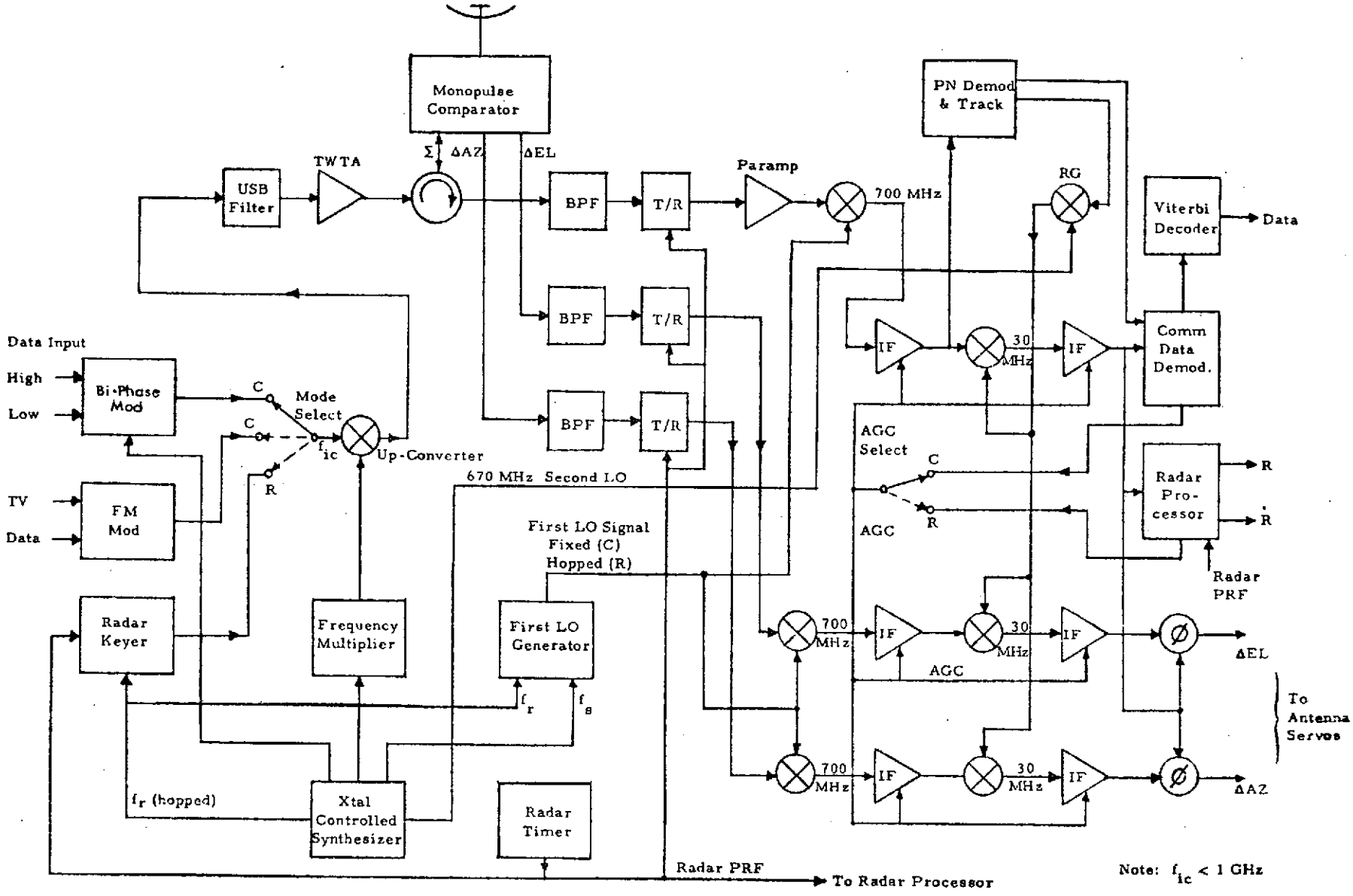


Figure 4. Integrated Ku-Band Radar/Communications System

importance to radar operation. For the communication mode, the crystal control minimizes frequency drifts of the transmit and receive signals.

Consider first the transmitter portion of the overall system. As shown, both the communication and the radar modulation are developed at intermediate carriers ($f_{ic}$) below 1 GHz and then these modulated carriers are up-converted to their final Ku-band frequencies. This translation is accomplished by mixing with a fixed LO frequency and by selection of the upper sideband (USB) of the mixer output. The filtered signals are then amplified by a wideband TWT amplifier to a maximum power level of approximately 40 watts. The output of the TWT amplifier is then applied via a circulator to the transmit terminal of the common antenna. It must be noted, that, although no filter is shown at the output of the TWT, filtering may be ultimately required to prevent TWT noise from degrading the noise figures of the receivers. The exact implementation of such a filter, or filters, will depend on the noise characteristics of the tube and the degree of isolation between the transmit and receive channels.

In the radar mode, both the RF drive signal and the TWT's grid are keyed to prevent spurious transmitter radiation during the receive cycle. In the communication mode, the transmitted signal is continuously on (CW) and it carries either an analog FM modulation (with a subcarrier for digital data) or a 50 Mbps bi-phase modulation.

The receive portion of the system consists of three receivers; (a) the sum channel, (b) the $\Delta$AZ, and (c) the $\Delta$EL channels. Based on the assumption that the radar frequency is within the bandwidth of the parametric amplifier, the sum signal amplification is accomplished in a common channel which thus benefits from the low noise figure of the parametric amplifier.

As shown in the block diagram, the receivers use double conversion to develop a sufficient amount of stable gain. The first IF is at 700 MHz and the second IF is at 30 MHz. These frequencies are compatible with

signal bandwidths at various points and, being standard frequencies, provide for component availability.*

The first local oscillator (LO) frequency is fixed for the communication mode and is frequency hopped for the radar mode. The hopped LO signal is derived in such a manner that its frequency hops are identical to the hops of the radar transmit signal. This can be implemented by first mixing the radar excitation frequency, $f_r$, with a Ku-band signal ($f_3$) derived from the synthesizer and then selecting the proper sideband of the mixer product. This operation is performed by the LO generator which may be a part of the synthesizer.

The second LO signal of 670 MHz is also derived from the synthesizer. In the communication mode, the second LO signal is bi-phase modulated with the PN code used for spectrum despreading. This signal is generated in the reference generator mixer, RG. Note that, in the communication mode and in the absence of the beacon, spectrum despreading is performed not only in the sum communication channel but also in the AZ and EL error receiver channels. For the radar mode, the RG mixer is turned on in such a manner that only a CW second LO signal is applied to the second mixers.

The 30 MHz IF signal of the sum channel is applied to the radar and the communication processors. It is also used as the phase reference for the angle tracking phase error detectors. Because the AGC requirements for radar and communication modes are different, the AGC control lines to the first and second IF amplifier chains are fed by signals generated by either the radar or the communication processors, respectively.

Figure 5 shows the block diagram for the Second IF Amplifiers and Demodulators/Detectors portion of the Integrated Radar/Communications Ku-Band system. Functions performed by the subunits of this block diagram are described below.

---

*This IF selection is typical, but not necessarily final.

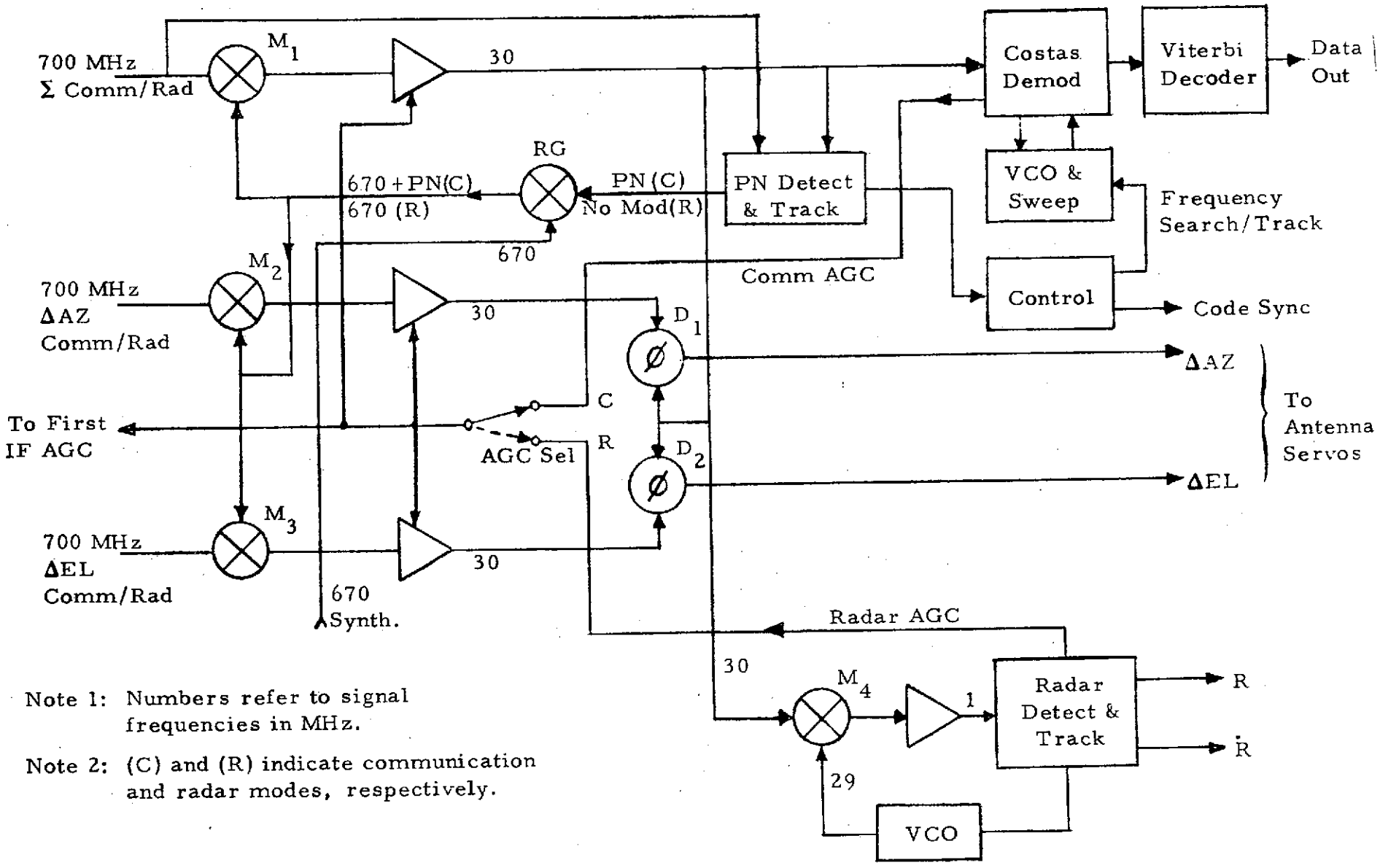


Note 1: Numbers refer to signal frequencies in MHz.

Note 2: (C) and (R) indicate communication and radar modes, respectively.

Figure 5. Radar/Communications System Second IF Amplifiers and Demodulators/Detectors

Radar Mode

The 700 MHz sum and angle track error signals are converted to the second IF of 30 MHz in mixers $M_1$, $M_2$, and $M_3$, respectively. The second local oscillator signal of 670 MHz is provided by the coherent synthesizer which, as was previously mentioned, is a common unit of the integrated system. In the radar mode, this signal is passed through the RG mixer without modulation and applied to the LO terminal of mixers $M_1$, $M_2$, and $M_3$.* The amplified sum channel radar return is then applied to $M_4$ where it is further converted to the third IF of about 1 MHz. Thus, in the radar mode, triple conversion is used to obtain an IF signal whose frequency is low enough to be used with all digital processing if such processing is selected to implement multiple filter detectors for the initial doppler acquisition.

The amplified 30 MHz sum channel radar return is also applied as a reference signal to the azimuth and the elevation phase error detectors $D_1$ and $D_2$, respectively. These detectors recover phase and amplitude of angle track error signals amplified by separate IF channels which follow mixers $M_2$ and $M_3$. The two error amplifier channels are shared between the radar and the communication modes. However, because the dynamic range of radar and communication signals is different, the AGC control signals are switched for the two modes. The operation of the radar detector and tracking unit is described in detail in Reference 1.

Communications Mode

In the communications mode, the 700 MHz first IF signals carry, in addition to the data stream, the spread spectrum PN modulation which may be typically clocked at rates between 11 and 14 Mbps. Thus, to remove this modulation from the 30 MHz second IF signals, the 670 MHz second LO signal is bi-phase modulated by a locally generated replica of the PN

---

*NOTE: If gating of both the first and second LO signals will be required to provide sufficient signal suppression during the radar transmit cycle, such gating can be conveniently applied to the RG mixer.

code. This modulation takes place in the reference generator mixer, RG. Note that, because the angle tracking is performed on the communication signal rather than the beacon signal, the removal of the spread spectrum PN signal is also performed in the angle tracking channel mixers $M_2$ and $M_3$.

Coherent demodulation of the bi-phase communication data is performed by the Costas loop, whose output is first applied to a symbol synchronizer and then to a Viterbi decoder. The function of the PN Detect and Track subunit is to search out, during the initial acquisition, the proper phase of the received code and subsequently to keep the phase of the local PN code in synchronization with the phase of the received code. Once the code phase coincidence is detected, the control unit performs the frequency search with the Costas loop's VCO until the carrier sync is established.

### 4.2.2 Communication Signal Acquisition and Tracking

#### Boresight Acquisition and Tracking

The first step in acquiring the communication signal is to detect the condition when the Orbiter's antenna is pointed directly at the TDRS. Assuming that the TDRS antenna is already pointed at the Orbiter, the latter's antenna still has to be scanned over the solid angle defined by the residual designation error. The boresight condition is then declared when the output of the communication receiver is either at its maximum or exceeds a certain threshold. If a special beacon signal is available, the boresight detection and subsequent angular tracking is performed with this signal. But if such a signal is not provided, as in the case considered, boresight detection and angle tracking must be performed using the communication signal itself. The following quantitative example shows that angular acquisition and tracking is possible using the downlink communication signal.

Consider first the boresight detection. Because such detection takes place prior to PN synchronization, the detection must be performed by an

envelope detector and in the bandwidth approximately equal to the PN code rate. Let us assume that this bandwidth is 12 MHz.

The downlink power budget, assuming circular polarization of the Orbiter's antenna, indicates that there is a net $P_{rec}/N_o$ of about 72 dB-Hz available at the Orbiter's receiver. The detection bandwidth of 12 MHz is equivalent to about 71 dB-Hz. Thus, net signal-to-noise ratio at the input to the envelope detector is

$$\text{SNR (in 12 MHz)} = 72 \text{ dB-Hz} - 71 \text{ dB-Hz} = 1 \text{ dB} .$$

The number of samples of the wideband envelope detected signal which have to be integrated to yield a required probability of detection and false alarm rate can be determined from a set of curves given in Chapter 2 of Reference 2.

Let the probability of detection $P_d$ be equal to 0.95 and the false alarm probability $P_{fa}$ be equal to $10^{-10}$. From Figure 8, page 2-21 of Reference 2, for input SNR = 1 dB, the number of pulses integrated to obtain these $P_d$ and $P_{fa}$ is about 70.

Since the sample duration is approximately equal to the inverse of the bandwidth, the total integration time is approximately equal to the number of pulses integrated, N, divided by bandwidth, B.

$$t_{int} = \frac{N}{B} = \frac{70}{12\times10^6} = 5.8\times10^{-6} \text{ sec or } 5.8\,\mu\text{sec} .$$

The corresponding false alarm time is approximately

$$t_{fa} = \frac{N}{B P_{fa}} = \frac{70}{12\times10^6 \times 10^{-10}} = 5.8\times10^4 \text{ sec} .$$

The integration time appears negligible compared to the rate at which the antenna may be stepped from one search position to another. Therefore, the actual time to scan over the designation uncertainty angle will depend on the characteristic of the antenna servo loop and the scan program

selected. The important fact is that the false alarm time far exceeds the minimum requirement of 10 minutes.

Consider now the magnitude of the residual rms angular fluctuation which will exist in the antenna servo loop if angular tracking is done on the communication data signal. The basic data rate of this signal (downlink) is about 1 MHz. The rate 1/3 coding increases this rate to about 3 MHz and, furthermore, the Manchester coding approximately doubles this rate. Thus, one requires at least 6 MHz bandwidth to accommodate the downlink signal. If one includes the doppler uncertainty of about $\pm 0.5$ MHz, the bandwidth requirement is increased to 7 MHz. This is equivalent to 68.5 dB-Hz. The signal-to-noise ratio in this bandwidth is then:

$$\text{SNR (7 MHz)} = 72 \text{ dB-Hz} - 68.5 \text{ dB-Hz} = 3.5 \text{ dB} \qquad (2)$$

or a ratio of 2.25.

The rms angular tracking error is defined by the expression

$$\sigma_\theta = \frac{\Theta_B \text{ (3 dB)}}{K_m \sqrt{(S/N)_{if} B_{if}/B_n}} \qquad (3)$$

where $\sigma_\theta$ = rms error

$\Theta_B$ (3 dB) = 3 dB antenna beamwidth

$K_m$ = antenna error slope (typically 1.5)

$B_{if}$ = IF bandwidth

$B_n$ = servo noise bandwidth (typically $\leq 10$ Hz)

$$\sigma_\theta = \Theta_B \frac{1}{1.5 \sqrt{(2.25)(7\times10^6/10)}} = \Theta_B \times 0.51 \times 10^{-3} \text{ degrees} \qquad (4)$$

Thus, one concludes that even with a 7 MHz wide signal, the angular tracking error is a small fraction of the 3 dB antenna beamwidth. The

$\sigma_\theta$ value computed in equation (4) may be somewhat optimistic because it does not take into account various signal suppression effects which take place at low signal-to-noise ratios. However, there appears to be adequate margin to allow for these effects.

PN Code Acquisition and Tracking

The PN code acquisition is the next step after completion of the angular search. This function, as well as PN code tracking after acquisition, is performed by circuitry shown in the block diagram of Figure 6.

To detect code phase coincidence, the local reference coder is clocked at a rate which is different from the normal clock rate. This makes the phase of the PN code applied to the reference generator mixer slide past the phase of the received code. When the phase difference is within one code bit, the data signal will appear at the output of the second IF sum channel. The bandwidth of this signal is determined by the data rate but it is narrower than the bandwidth of the spread spectrum signal. Thus, the output of the second IF bandpass filter (BPF) is applied to a noncoherent detector (rectifier)* and, after low pass filtering (post detection integrator), it is applied to a threshold detector. When the code phase coincidence is such that a preset post detection integration threshold is exceeded, code sync is declared and the PN detector is switched into the track mode.

As shown in Figure 6, code tracking is performed by the Early/Late correlators. The outputs of these correlators are centered at the 30 MHz second IF frequenty and, consequently, have to be bandpass filtered and rectified prior to subtraction. The subtraction produces the composite response which minimizes the tracking error when the incoming and local reference codes are in phase. The loop filter provides post detection integration and will be optimized to accommodate the Orbiter dynamics with respect to the TDRS satellites.

---

*Labeled as "ABS" in Figure 6.

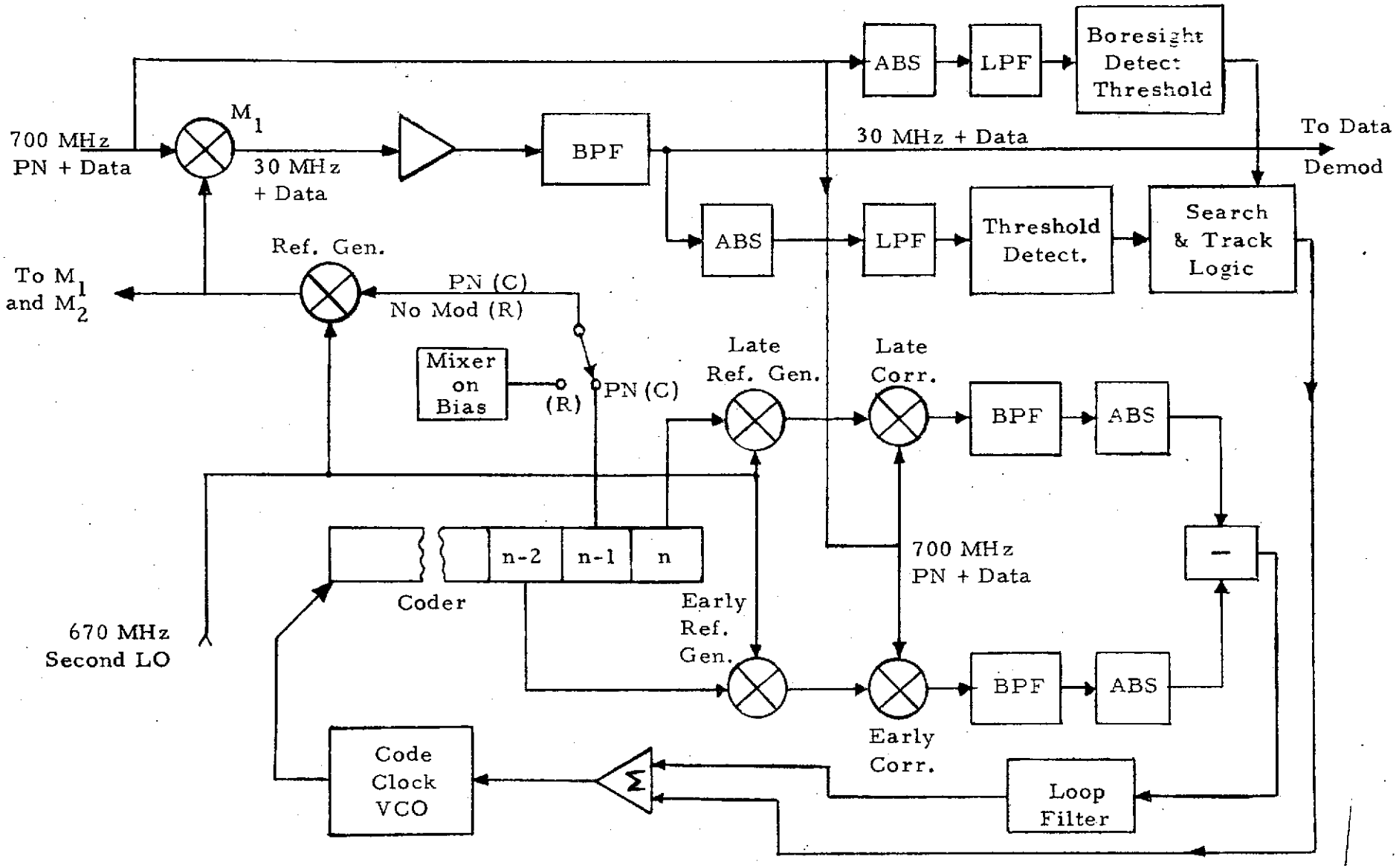


Figure 6. PN Code Detector and Tracker

Ideally, the bandwidth of the bandpass filters which follow the early/late correlators should be matched to the data rate. However, because doppler rates of up to $\pm$400 kHz are expected, this bandwidth may be widened to accommodate the doppler shift.

The PN acquisition time is quite small. Using the implementation shown in Figure 6 with sequential detection, Table VII summarizes the PN acquisition time for probability of detection $P_d = 0.9$ and false alarm rate greater than 10 minutes. The design point for probability of bit error of $10^{-6}$ is 5 dB. Thus, with no circuit margin, the average time to sync is 10 milliseconds and sync is achieved in 90 percent of the trials by 20 milliseconds. At extremely low signal strength, such as $E_b/N_o = 0$ dB, corresponding to a bit error probability of $10^{-1}$, the average PN sync time is only 0.13 seconds and sync is achieved in 90 percent of the trials by 0.3 seconds. Thus, PN acquisition is not considered to be a problem area.

TABLE VII

PN SYNCHRONIZATION TIME FOR $P_d = 0.9$

| $E_b/N_o$ (dB) | Average Sync Time (sec) | Time to Achieve Sync in 90% of Trials (sec) |
|---|---|---|
| 0 | 0.13 | 0.30 |
| 5 | 0.01 | 0.02 |

# V. MODULATION/CODING DESIGN FOR COMMUNICATIONS

The basic design approach for the Orbiter wideband relay link is as follows. In order to accommodate television or scientific data in analog form, the efficiency and hardware simplicity associated with frequency modulation dictate that an FM modulator be used. However, in order to accommodate digital data rates on the order of 50 Mbps (under the power constraints which are present using a 20-inch antenna and a 40-watt transmitter at Ku-band), the use of coded (rate 1/2, constraint length 7 convolutional coding), coherent PSK appeared obvious.

Consequently, both a PSK and an FM system are planned for use on the Orbiter, and it will be necessary to switch between these systems to accommodate the various possible signals to be transmitted. The complexity associated with two switched demodulation/detection systems must also be imposed on the ground station equipment.

The desirability of a single transmitting/receiving system for the Shuttle wideband data relay links is evident, since a savings in both spaceborne and ground hardware could be realized and the reliability of the overall ground system could be increased. The most attractive approach would be to utilize the FM modulator for all possible input signals, including the wideband digital (up to 50 Mbps) signals. Subsequent sections consider various ways in which the FM modulator could be used for transmission of digital data. Both binary and M-ary FSK have been examined [14] and the potential use of coding in conjunction with either of these modulation techniques is discussed. Use of both coherent and noncoherent detection schemes at the ground station are examined. However, further study is necessary, including breadboard testing, before the performance of the binary and M-ary modulation schemes with coding is established under a practical environment. Therefore, these modulation schemes are not baselined for the Ku-band communication system at this time.

## 5.1 Baseline Signal Design for Communications

To meet the communication requirements presented in Section II, quadrature PSK modulation is baselined for wideband digital data. This modulation scheme has been thoroughly tested [15] and there is confidence in specifying the system performance. Therefore, for the forward link, up to 1 Mbps of wideband data is quadrature PSK modulated with 72 kbps of operational data (8 kbps of encoded commands plus sync, and two 32 kbps voice channels). For the return link in Mode 1, up to 50 Mbps of wideband digital data is quadrature PSK modulated with up to 2 Mbps digital data (real time 192 kbps operational data or playback of recorded operational data from maintenance/loop recorders or playback from experiment PCM recorder or real time experiment data). For the return link in Mode 2, up to 2 Mbps digital data (playback of recorded operational data from the maintenance/loop recorders or playback from experiment PCM recorder or real time payload data) is quadrature PSK modulated with the 192 kbps operational data on a subcarrier of approximately 8 MHz. The quadrature modulated digital data on the subcarrier is frequency modulated with either wideband analog up to 4.2 MHz (television or payload analog data) or up to 4 Mbps payload digital data.

Figure 7 presents the proposed modulator and demodulator for the Mode 2 return link. As shown in Figure 7a, the output of the 8 MHz subcarrier is split into two components which are shifted 90 degrees with respect to each other. One component, labeled as "0-degrees," is applied to balanced modulator BM 1 where it is bi-phase modulated with the 192 kbps data stream. Similarly, the "90-degree" subcarrier component is applied to balanced modulator BM 2 where it is bi-phase modulated with the 2 Mbps data stream.

The outputs of BM 1 and BM 2 are summed to form a quadriphase modulated subcarrier. Attenuation pads (or gain controls) are provided at the outputs of the balanced modulators to provide for proper power division between the two components of the quadriphase subcarrier.

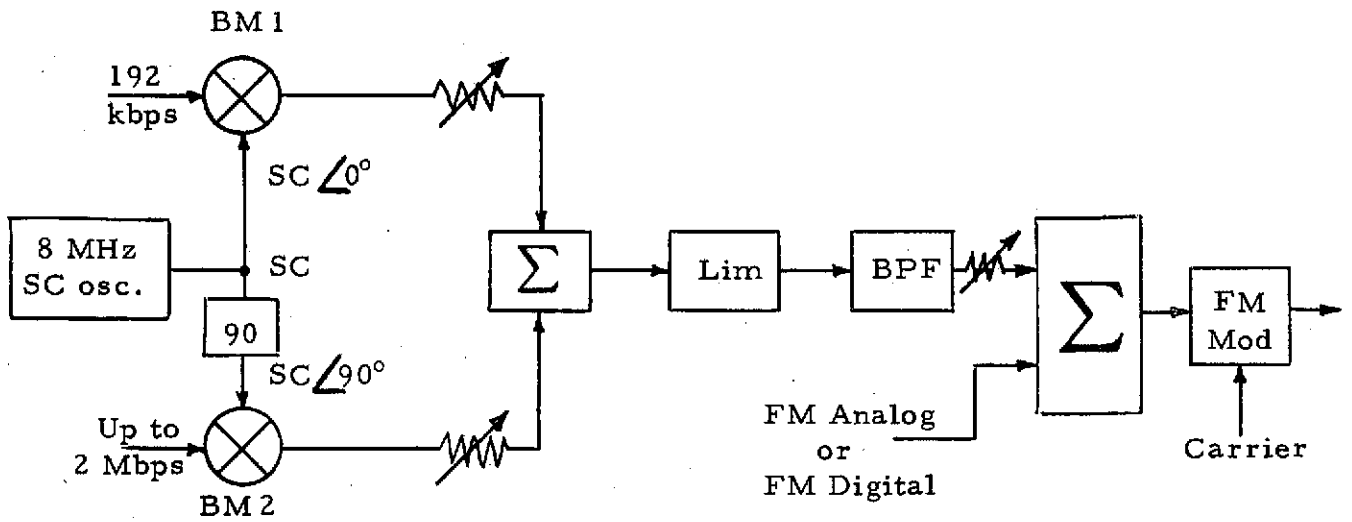


(a) Modulator

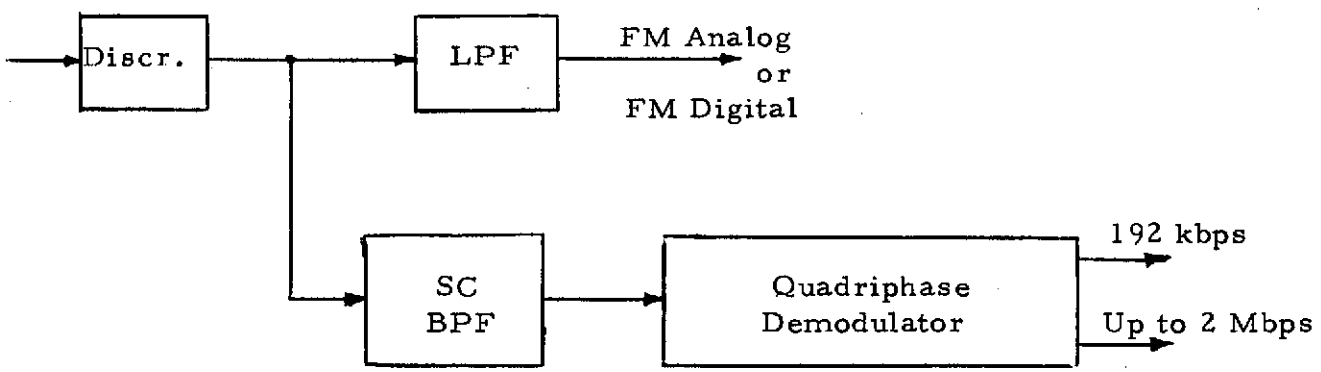


(b) Demodulator

Figure 7. Modulator and Demodulator for Mode 2 Return Link

The quadriphase subcarrier is then hard limited to provide a constant envelope signal and passed through a bandpass filter which prevents the splattering of the subcarrier spectrum into the baseband analog or digital data. The subcarrier is then, after proper weighting, linearly added to the baseband analog or digital data and the combined signal is applied to an analog FM modulator.

Figure 7b shows the corresponding demodulator. As shown, this demodulator consists of a discriminator whose output is split into the baseband and subcarrier channels. The subcarrier channel is demodulated by a quadriphase demodulator of the type described in detail in Reference 15. The salient feature of the quadriphase demodulator configuration referenced is that it can handle two independent data streams which can be of widely different asynchronous rates and can be of different power levels.

## 5.2 Baseline Coding for Wideband Digital Data

Convolutional encoding with Viterbi decoding is used on all links that require channel error control because of the favorable trade-off between performance and complexity offered by this coding technique. On the forward link, a rate 1/3, constraint length K = 7 will be used. This coding is similar to that used on the S-band communication links and therefore the performance and implementation complexity have been established. For the return link, a rate 1/2, constraint length K = 7 will be used for the 50 Mbps wideband digital data. At 50 Mbps, convolutional encoding and Viterbi decoding become difficult and require further study to establish the system performance and complexity. The most feasible technique for the 50 Mbps Viterbi decoder is to use five 10 Mbps Viterbi decoders in parallel as shown in Figure 8. The 10 Mbps Viterbi decoders have been implemented by Linkabit and therefore would not require development. While the decoders are on the ground and complexity is not as critical as on the Orbiter, convolutional encoding at 50 Mbps is also complex and may require up to 100 ICs.

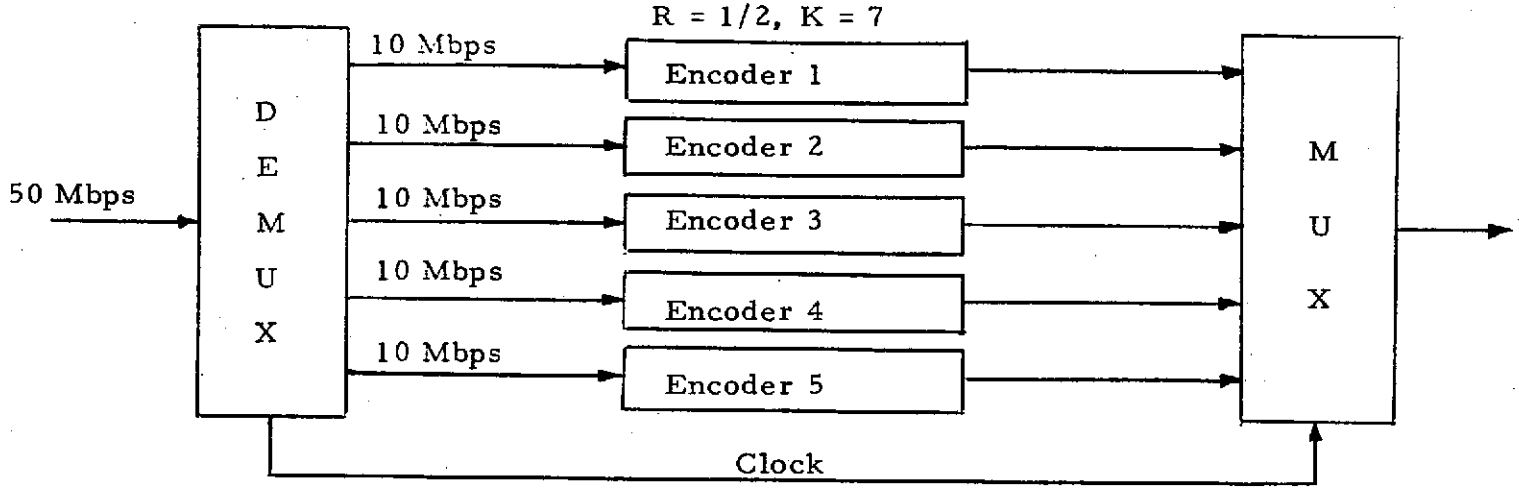


ORBITER 50 MBPS ENCODER

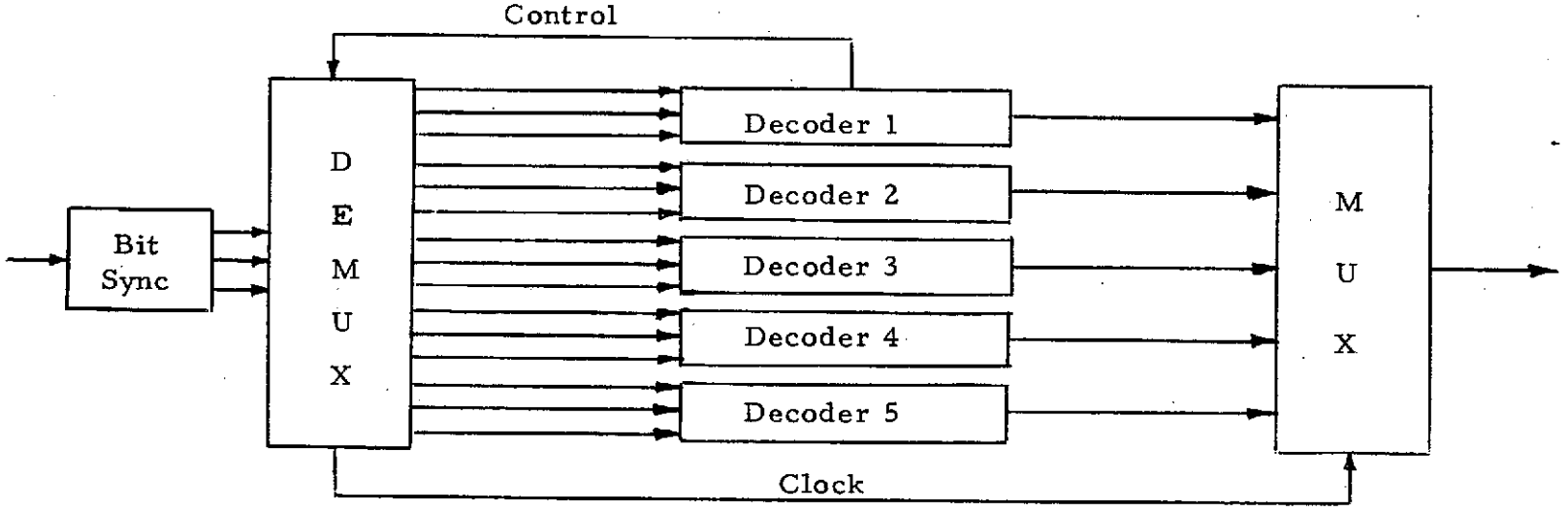


GROUND 50 MBPS DECODER

Figure 8. Convolutional Encoding and Viterbi Decoding at 50 Mbps

## 5.3 Alternate Modulation/Coding Techniques

The modulation schemes to be considered alternatives to coded coherent PSK are binary frequency shift keying (BFSK) and M-ary or multiple frequency shift keying (MFSK) with either coherent or noncoherent detection. First, uncoded results are presented, then the coded results.

### Uncoded BFSK

The simplest alternative to PSK is BFSK in which the digital information is related by one of two different carrier tones. These tones can either be coherently related (derived from one oscillator as in FM modulation) or they can be noncoherently related (derived from two independent oscillators). In the coherently related case, the two resulting signals can either be correlated (with negative correlation) or uncorrelated (orthogonal). Finally, detection proceeds either with or without knowledge of the carrier phase.

First, consider the reception in Gaussian noise of two signals with coherently related frequencies. These signals are described by

$$s_0(t) = \sqrt{2S}\cos\left(\omega t + \frac{\pi h}{T}t + \theta\right)$$

$$s_1(t) = \sqrt{2S}\cos\left(\omega t - \frac{\pi h}{T}t + \theta\right), \quad 0 \le t \le T, \tag{5}$$

where S is the average signal power, $h = 2f_d T$ is the frequency deviation ratio, and $f_d$ is the deviation frequency. The normalized correlation $\rho$ between these two signals is easily shown to be

$$\rho = \frac{\sin 2\pi h}{2\pi h}. \tag{6}$$

The optimum coherent detector for these signals is shown in Figure 9. The bit error probability for this detector is given by [16]:

$$P_B = Q\left(\sqrt{(1-\rho)\, E_b/N_o}\right) \tag{7}$$

where $E_b = s/T$ and $Q(\cdot)$ is defined by

$$Q(x) = \frac{1}{\sqrt{2\pi}} \int_x^\infty e^{-t^2/2}\, dt \ . \tag{8}$$

From (7), the minimum value of $P_B$ for a given $E_b/N_o$ is obtained when $\rho$ is minimized. The minimum value of $\rho$ from (6) is $\rho = -0.22$ when $h = 0.715$. Thus, the optimum probability of error is given by

$$P_B = Q\left(\sqrt{1.22\, E_b/N_o}\right) \ . \tag{9}$$

Equation (9) is plotted in Figure 10 versus $E_b/N_o$. Note that this performance is 2.2 dB worse than PSK.

Next, the noncoherent reception of the signals in (5) via a conventional discriminator detector was considered [17] as shown in Figure 11. This model was recently studied by Tjhung and Wittke [18] who showed that there existed an optimum predetection filter bandwidth and an optimum deviation ratio. Their computation of the probability of error for this system is also plotted in Figure 10. Note that, for small error rates ($< 10^{-4}$), this performance is 2.5 dB worse than PSK or only 0.3 dB worse than the optimum BFSK.

Finally, consider the reception of two signals with noncoherently related frequencies. These are described by

$$\begin{aligned} s_0(t) &= \sqrt{2S}\, \cos(\omega_1 t + \theta_0) \\ s_1(t) &= \sqrt{2S}\, \cos(\omega_2 t + \theta_1), \quad 0 \le t \le T \ . \end{aligned} \tag{10}$$

In this case, the signals are uncorrelated or orthogonal, since the two phases, $\theta_0$ and $\theta_1$, are uncorrelated. The optimum detector for this

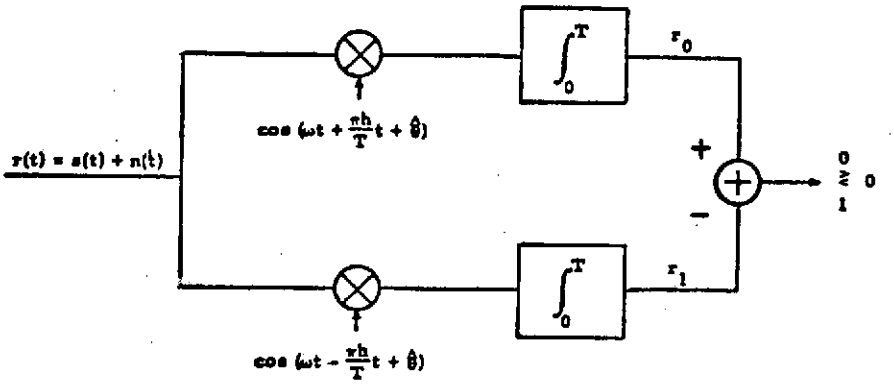


Figure 9. Optimum Coherent Detector for BFSK

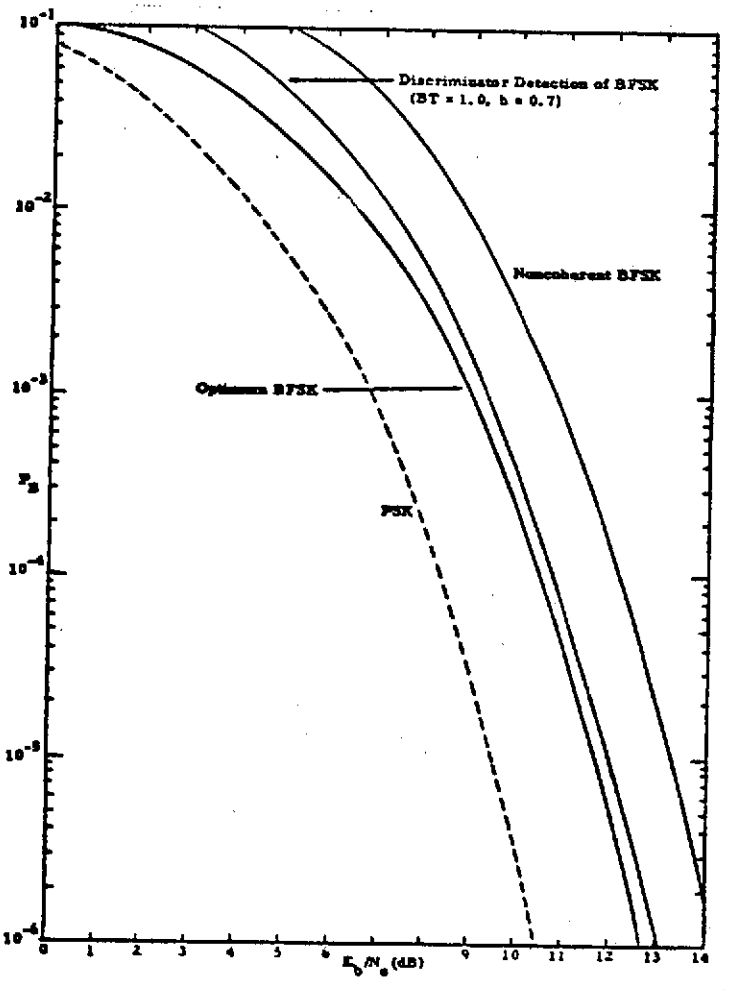


Figure 10. Performance of Various BFSK Schemes

system is the noncoherent detector shown in Figure 12. The bit error probability is given by [16]:

$$P_B = 1/2 \exp(-E_b/2N_o) \tag{11}$$

and this function is plotted in Figure 10. Note that this performance is very poor in comparison with all other schemes.

Uncoded MFSK

A generalization of BFSK is MFSK, in which n bits of information are transmitted via one of $M = 2^n$ different carrier frequencies. First, suppose the frequencies are coherently related, i.e.,

$$\begin{aligned} s_0(t) &= \sqrt{2S}\cos(\omega t + \omega_0 t + \theta) \\ s_1(t) &= \sqrt{2S}\cos(\omega t + \omega_1 t + \theta) \\ &\vdots \qquad\qquad 0 \le t \le T \\ s_{M-1}(t) &= \sqrt{2S}\cos(\omega t + \omega_{M-1} t + \theta) \end{aligned} \tag{12}$$

Furthermore, suppose the signals in (12) are mutually orthogonal. This implies that the frequencies are related by

$$(\omega_i - \omega_j)T = (i - j) \quad . \tag{13}$$

Then the optimum coherent detector for this scheme is shown in Figure 13. The bit error probability of this scheme is given by [16]:

$$P_B = \frac{2^{n-1}}{2^n - 1} P_E$$

$$P_E = 1 - \int_{-\infty}^{\infty} \frac{\exp(-t^2/2)}{\sqrt{2}} \left[1 - Q\left(t + \sqrt{2E/N_o}\right)\right]^{M-1} dt \quad , \tag{14}$$

where $E = nE_b$. Figure 14 shows (14) plotted versus $E_b/N_o$ for various

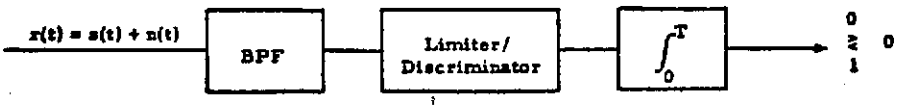


Figure 11. Discriminator Detector for BFSK

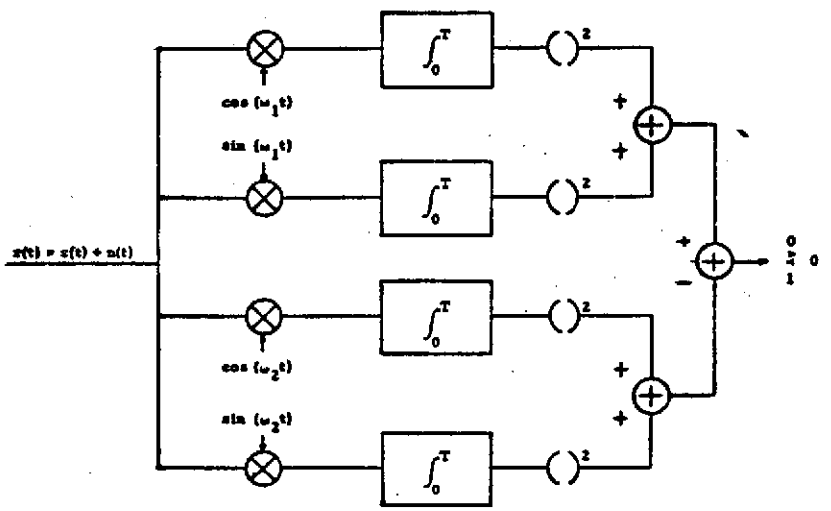


Figure 12. Optimum Noncoherent Detector for BFSK

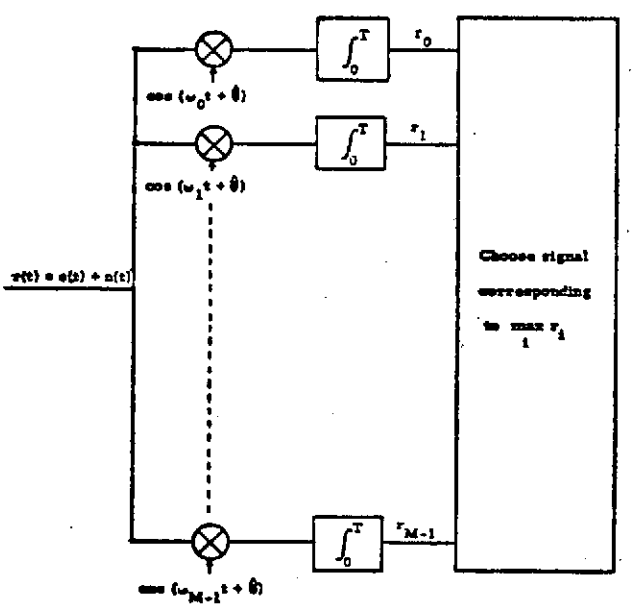


Figure 13. Optimum Coherent MFSK Detector

values of M. Note that the performance for M = 4 is only slightly worse than PSK, while M = 8 performs better than PSK for $P_B < 2\times10^{-1}$.

Next, suppose the M frequencies are noncoherently related, i.e.,

$$\begin{aligned} s_0(t) &= \sqrt{2S}\ \cos(\omega_0 t + \theta_0) \\ &\vdots \\ s_{M-1}(t) &= \sqrt{2S}\ \cos(\omega_{M-1} t + \theta_{M-1}), \quad 0 \le t \le T \ . \end{aligned} \tag{15}$$

Once again, the signals are (necessarily) mutually orthogonal. The optimum detector for this scheme is the noncoherent detector shown in Figure 15. The bit error probability is given by [19]:

$$P_B = \frac{2^{n-1}}{2^n - 1} P_E$$

$$P_E = \frac{\exp(-E/N_o)}{M} \sum_{j=2}^{M} (-1)^j \binom{M}{j} \exp(E/jN_o) \ . \tag{16}$$

Equation (16) is plotted in Figure 16. Note that the performance for M = 8 is better than PSK for $P_B < 10^{-3}$.

Coded BFSK

Now consider coding in conjunction with BFSK. The outputs of, say, the R = 1/2, K = 7 convolutional code are transmitted via the signals in (5) with h = 0.715. The coherent detector (shown in Figure 9) computes the decision statistics $r_0$ and $r_1$ for each received symbol. It can be shown that the log of the likelihood of $(r_0, r_1)$ being received, given that $s_0(t)$ was sent, is proportional to $r_0$. Similarly, the log of the likelihood of $(r_0, r_1)$ being received, given that $s_1(t)$ was sent, is proportional to $r_1$. Thus, $r_0$ and $r_1$ form the basic symbol metrics for a soft decision Viterbi decoder. It is easy to estimate the performance of this system since the channel statistics are almost the same as those of a PSK channel.

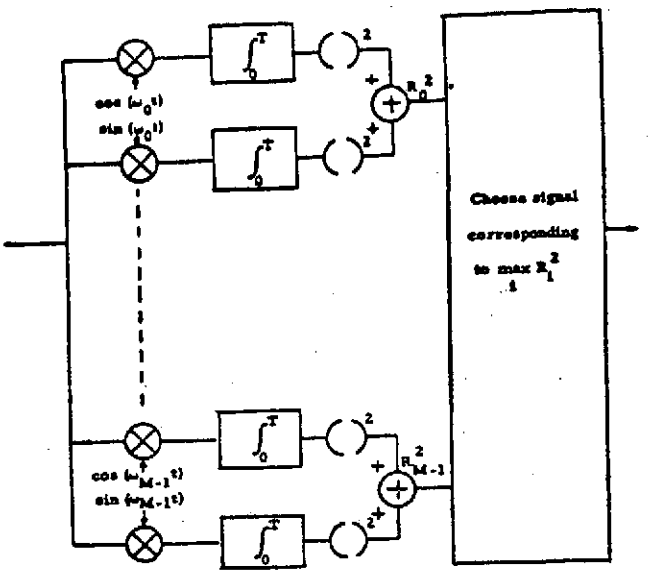


Figure 15. Optimum Noncoherent MFSK Detector

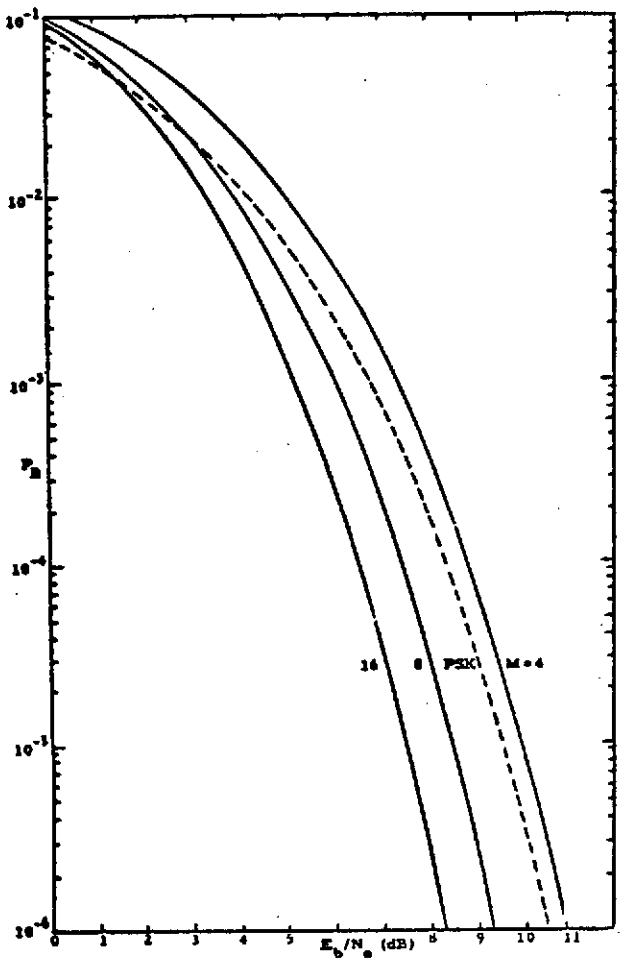


Figure 14. Performance of Coherent MFSK

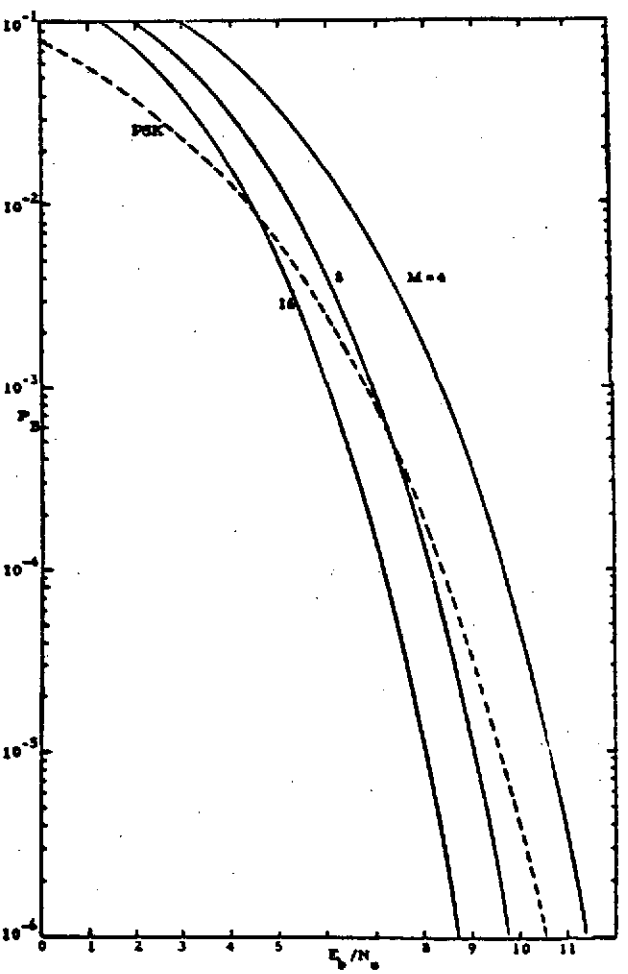


Figure 16. Performance of Noncoherent MFSK

Recall from Figure 10 that the uncoded $P_B$ for this channel was shifted by 2.2 dB from the PSK curve. Thus, the coded performance will be shifted by 2.2 dB also. This coded performance curve is shown in Figure 17.

A coded BFSK system with discriminator detection would be interesting; however, the analysis of such a system is mathematically intractable. Nevertheless, a good estimate of performance can be made in the following way. Coded systems usually operate on uncoded data whose probability of symbol error is between $10^{-1}$ and $10^{-2}$. For this region, the performance of the discriminator, from Figure 10, is between 3 and 4 dB worse than PSK. Thus, the coded performance with discriminator detection should be around 3 to 4 dB worse than coded PSK.

Coded MFSK

Of all the candidate modulation schemes described above, orthogonal MFSK with either coherent or noncoherent detection seems to be the most promising from a probability of error standpoint. The question is how to apply coding to this type of modulation. One might consider sending each set of n code symbols as one of $2^n$ signals, but at the receiver, a hard decision must be made on the received signals so that the binary Viterbi decoder can process the individual symbols. This scheme, of course, does not use the full information available; that is, it does not use soft decisions.

Another approach, proposed in [20] and generalized in [21], is to use a nonbinary convolutional code. Figure 18 shows such a code with constraint length 7 and n adders. Each bit into the encoder produces n code symbols which are transmitted via one of $2^n$ orthogonal signals such as described by (12) or (15). This produces a linear tree code with one signal per branch as shown in Figure 19. At the receiver, the M statistics $r_0, r_1, \ldots, r_{M-1}$ are computed (see Figures 13 and 15). The basic branch symbol metrics used by the Viterbi decoder can be shown

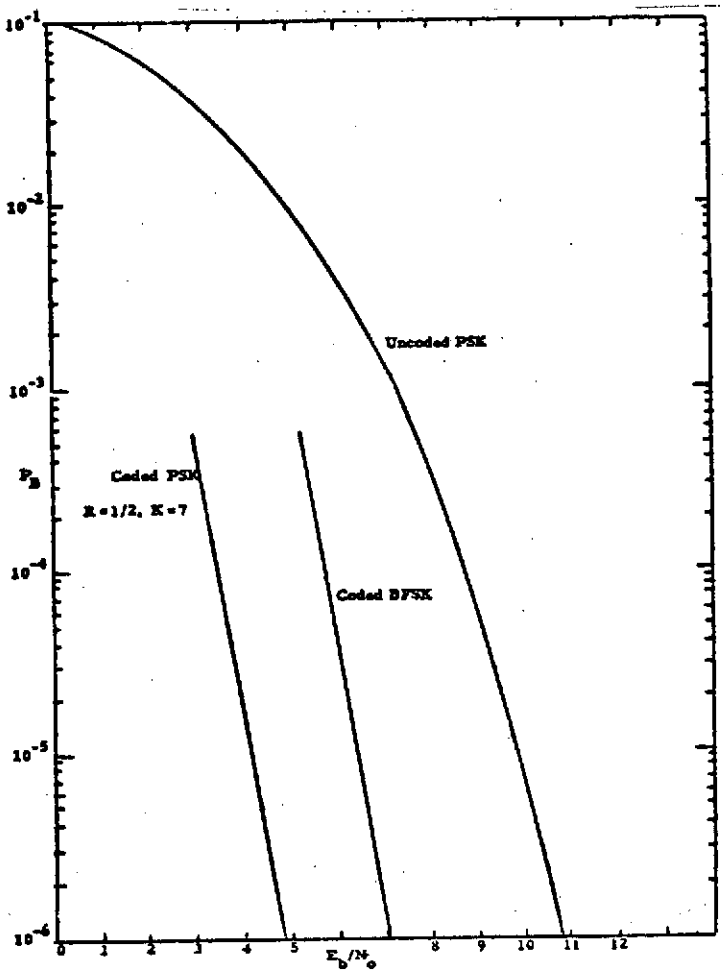


Figure 17. Performance of R = 1/2, K = 7 Code with Optimum Coherent BFSK

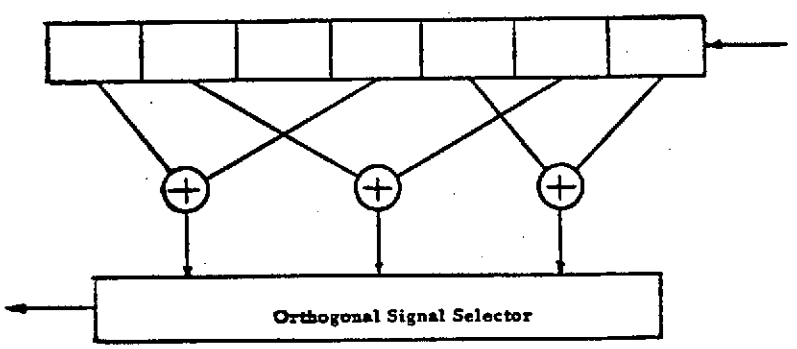


Figure 18. K = 7 Nonbinary Convolutional Encoder

to be

$$m_i = r_i \qquad \text{(coherent)} \tag{17}$$

$$m_i = \log I_0\left( r_i \sqrt{2E_b/N_o} \right) \qquad \text{(noncoherent)} \tag{18}$$

where $m_i$ is proportional to the likelihood of receiving $(r_0, \ldots, r_{M-1})$ given that the signal $s_i(t)$ was sent.

Upper bounds on the bit error probability for the coded system can be computed for both coherent and noncoherent reception [21, 22]. These bounds are essentially the weight structure union bounds introduced by Viterbi [23], except the weights in this case are different. For instance, the weight of the symbol corresponding to $s_0(t)$ is defined to be zero while the weight of all other symbols is one. Since the weight on a branch is then at most one, the maximum weight that the minimum weight path can have (the free distance, $d_f$) is K, the constraint length of the code. This leads to the question of optimum codes for M-ary systems. For example, the R = 1/2, K = 7 binary code has maximal $d_f = 10$. When used in conjunction with 4-ary modulation, the free distance of this code is 6, or one less than the maximum possible. Thus, optimum binary codes are not necessarily optimum nonbinary codes. For this reason, an exhaustive search was made for the best code to be used with 8-ary modulation [24]. The code found had $d_f = 7$ and it gave the smallest probability of error for a large range of $E_b/N_o$. The performance of this code with both coherent and noncoherent detection is shown in Figure 20. Note that the coherent performance is within 0.4 dB of the baseline PSK system.

The results of this study indicate that a coded M-ary FSK system can indeed be competitive with coded coherent PSK for the Shuttle wideband data relay communications link. A coherent detection scheme should be used, but the associated hardware complexity will be at the ground station. A coded (R = 1/3, K = 7) 8-ary FSK design, which appears to

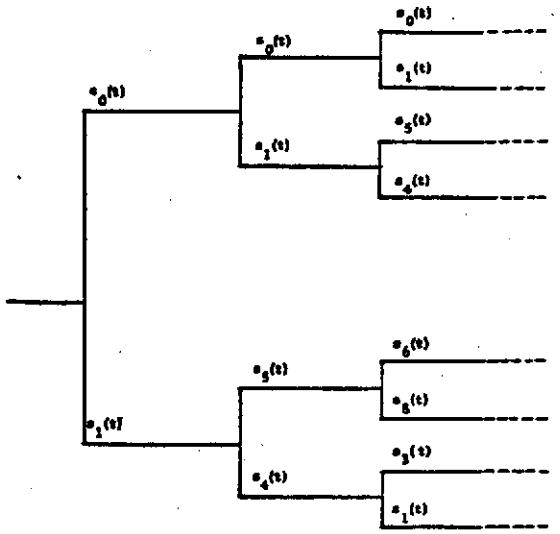

Figure 19. Nonbinary Orthogonal Tree Code

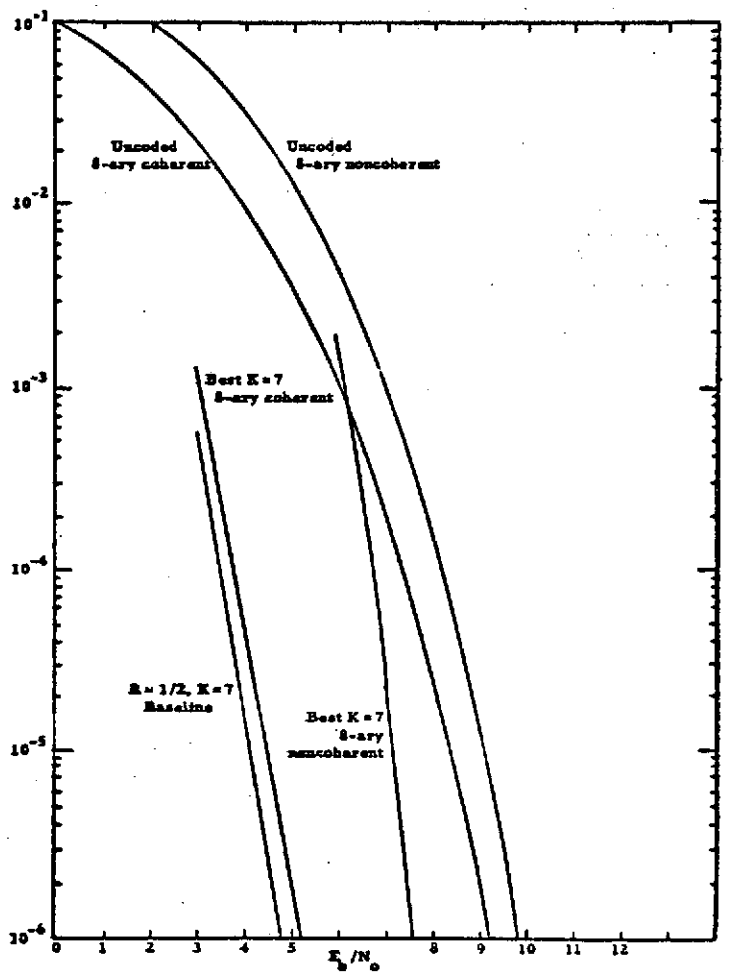


Figure 20. Performance of Coded Coherent and Noncoherent MFSK

offer the best compromise between performance and complexity, was shown to perform only slightly worse (0.4 dB) than the coded (R = 1/2, K = 7) binary PSK design which was tentatively chosen for the wideband relay link. This coded MFSK design must therefore be seriously considered as a potential replacement for the baseline design.

# VI. AREAS FOR FURTHER STUDY

A preliminary configuration for the Integrated Ku-Band Radar/ Communication System has been described in this report. There remain, however, several areas which require additional quantitative investigation to aid in making recommendations for the final system configuration. These areas are described below.

## 6.1 Angle Acquisition and Tracking

The inclusion of the parametric amplifier in the sum channel provides for improved sensitivity of the communication and radar system performance. However, this makes the sum receiver channel electrically different from the tracking error and receiver channels. The difference is that of gain and phase. The extra gain in the sum channel can be compensated for in the error channels by adding equal gains, except at IF, to these channels. The remaining question is that of differential phase shift through the paramp channel and the sensitivity margin in the error channels.

Preliminary considerations indicate that phase drift within the paramp may be relatively slow and thus a technique which provides for only a periodic compensation can be employed to take out paramp drifts when these drifts exceed allowed tolerances. Further study is necessary to determine if techniques for drift compensation are required.

An analysis of the required sensitivity for the azimuth and elevation channel receivers is needed. If additional sensitivity is required, consideration should be given to the use of parmetric amplifiers in these channels. However, because of the cost and additional complexity involved, the number of parametric amplifiers must be minimized. Techniques for sharing a single receive channel, including a paramp, between the two error channels can be used, however. Multiplexing of tracking errors is performed on a time-shared basis according to a preselected sample pattern. Following amplification in a common receiver channel, the errors are demultiplexed and their amplitudes and phases recovered by

phase sensitive detectors which utilize the output of the sum channel as a reference.

Techniques which provide for amplification of all three monopulse converter output signals, i.e., $\Sigma$, $\Delta$AZ and $\Delta$EL, in a single receiver channel are also available. Reference 25, for example, describes a technique for superimposing the tracking errors onto the sum channel directly at the output of the monopulse converter. Such RF combining permits all three channels to be processed by one common receiver, thus eliminating requirements for phase and gain matching between parallel channels. The greatest benefits which result from such single channel operation are, of course, system simplicity and low cost, because only one parametric amplifier is required.

The penalty paid for such single channel operation is typically a system loss of up to 1 dB with an accompanying increase in the overall system noise temperature. With an adequate system margin, this may be a reasonable penalty to pay for a significant system simplification.

A related area for further study is the effect of superimposing the angle track error signals on the sum channel which carries the communication data. Although the track error signals are typically much smaller than the sum channel signal, they may affect data performance, particularly at error rates in the $10^{-5}$ to $10^{-6}$ region. Thus, methods for minimizing the interchannel crosstalk need to be considered.

The system configuration described in this report is based on preliminary calculations which indicate that TDRS acquisition and angle tracking are possible, at least in principle, without a beacon signal. The capabilities and limitations of such an approach, however, remain to be summarized on a quantitative basis. Specifically, acquisition times for the range of conditions, as well as tracking accuracy limitations, must be determined quantitatively and compared to the beacon tracking conditions. If it is determined that beacon tracking rather than signal tracking is preferable, the impact of modifying the configuration described in this report for beacon tracking will have to be considered. Axiomatix has

already considered beacon tracking configurations in the past, and the impact of such modification is not expected to be severe. The main area of modification to accommodate beacon tracking, should such modification be found necessary, will be in the rearrangement of front end filtering, the IF bandwidth, and possibly an additional mixer.

## 6.2 Transmitter Filtering Requirements

Excessive splatter of the transmitter tube's output noise into the communication receiver channel may necessitate filtering of the transmitter output. The degree of filtering required will depend on the intrinsic isolation available between the transmitter tube and the receiver output as well as on the noise figure of the transmitter tube. The effect of separation between the communication transmit and radar frequency will also influence the degree of filtering required.

## 6.3 Performance Analysis of the Rendezvous Radar

Much of the analysis and optimization of the rendezvous radar was for the search mode, because the search mode determines the transmitter power required. Range rate tracking for the noncoherent radar has been studied. However, a more detailed analysis of the noncoherent radar may be required before the noncoherent radar could be considered for the baseline. Also, while less critical to the baseline selection, the doppler and range tracking of the coherent pulse doppler radar must be analyzed in detail to completely specify the coherent radar performance.

An important area for further study is the target effects on the radar performance. Effects such as target glint, scintillation, and extended targets must be analyzed. These effects are specially significant at short ranges where scintillation and glint are very large. Thus, frequency diversity will be virtually required in order to reduce these effects at short ranges. At short ranges, stationkeeping with extended targets may dictate a coherent pulse doppler radar. One of the reasons

for this is the ratio of target size to range becomes so large that the definition of range and capacity of measuring range comes into doubt. Therefore, a coherent pulse doppler radar with doppler tracking capability may be the only acceptable approach.

Finally, the commonality of the radar and communication systems must be carefully analyzed to determine trade-offs in weight, power, size, and cost for various integration techniques. The noncoherent pulse radar, where the commonality between the two systems is small, must be compared with the coherent pulse doppler radar, where there is a great amount of commonality. However, from the preliminary analysis, the coherent pulse doppler radar is the most promising for the integrated radar/communication system both from the standpoint of performance and from the standpoint of weight, power, size, and cost.

## 6.4 Communication Signal Design

The most important area for further study related to the baseline communication signal design is the implementation of the receiver and signal processor for the 50 Mbps coded digital data. Note that, with rate 1/2 coding, the rate that the bit synchronizer must handle is 100 Mbps. A bit synchronizer with the small degradation required for coded communication must be developed for the 100 Mbps rate. While the bit synchronizer is on the ground where weight, size, and power are not as critical, a detailed analysis of the acquisition and tracking capabilities is needed and a breadboard of the synchronizer will be necessary to establish the expected performance in a coded communication system.

On the Orbiter, the 50 Mbps convolutional encoder requires additional investigation to simplify its implementation. Also, if the alternate modulation schemes presented in Section V are to be considered, the modulators and demodulators need to be breadboarded and tested. From these tests, the expected performance in a practical system can be established for these modulation schemes.

# REFERENCES


1. C. L. Weber, "Optimization of Proposed Radar for the Integrated Ku-Band Radar/Communication System," Axiomatix Report No. R7408-5 (Under NASA Contract NAS 9-13467), August 22, 1974.

2. M. I. Skolnik, Radar Handbook, McGraw-Hill Book Co., 1970.

3. F. E. Nathanson, Radar Design Principles, McGraw-Hill Book Co., 1969.

4. S. Udalov, "Preliminary Overall System Configuration for the Integrated Ku-Band Radar/Communication System," Axiomatix Report No. R7408-4 (Under NASA Contract NAS 9-13467), August 22, 1974.

5. D. B. Leeson and G. F. Johnson, "Short-Term Stability for a Doppler Radar: Requirements, Measurements, and Techniques," Proc. IEEE, February, 1966.

6. M. J. Mum, "The Meaning and Measurement of Spectral Purity," Motorola Report, Communications Division, Chicago.

7. W. B. Offutt, "A Review of Circular Polarization as a Means of Precipitation Clutter Suppression and Examples," Proc. of NEC, Vol. XI, October, 1955.

8. C. L. Weber, "Analysis of an RCA Proposal for a Pulsed Doppler Radar for Space Shuttle," Axiomatix Report No. R7407-1 (Under NASA Contract NAS 9-13467), July 1974.

9. C. L. Weber, "On the Optimal Choice of Antenna Scan Overlap," Axiomatix Report No. R7409-3 (Under NASA Contract NAS 9-13467), September 20, 1974.

10. J. V. DiFranco and W. L. Rubin, Radar Detection, Prentice-Hall, 1968.

11. C. L. Weber, "Estimation of Range Rate for Noncoherent Radar," Axiomatix Report No. R7410-2 (Under NASA Contract NAS 9-13467), October 2, 1974.

12. R. S. Iwasaki, "TWT Study for Integrated Ku-Band Radar/Communication System," Axiomatix Report No. R7410-3 (Under NASA Contract NAS 9-13467), October 2, 1974.

13. "Tracking and Data Relay Satellite System (TDRSS) User's Guide," NASA Goddard Space Flight Center, Greenbelt, Maryland, June 10, 1974.

14. B. H. Batson, G. K. Huth, and B. D. Trumpis, "Coding/Modulation Trade-offs for Shuttle Wideband Data Links," to be presented at the National Telecommunications Conference, San Diego, California, December 1-4, 1974.

15. R. W. Allen and B.H. Batson, "A Variable-Data-Rate, Multimode Quadriphase Modem," in Proceedings of the 1973 International Conference on Communications, Seattle, Washington.

16. J. M. Wozencraft and I. M. Jacobs, Principles of Communication Engineering, John Wiley & Sons, Inc., New York, 1965.

17. B. D. Trumpis, "Optimum Parameters for the Space Shuttle Wideband Digital FM Direct Communication Link," Axiomatix Report No. R7406-1 (Under NASA Contract NAS 9-13467), June 4, 1974.

18. T. T. Tjhung and P. H. Wittke, "Carrier Transmission of Binary Data in a Restricted Band," IEEE Trans. Comm. Tech., August 1970.

19. A. J. Viterbi, Principles of Coherent Communication, McGraw-Hill Book Co., New York, 1966.

20. A. J. Viterbi, "Orthogonal Tree Codes for Communication in the Presence of White Gaussian Noise," IEEE Trans. Comm. Tech., April 1967.

21. B. D. Trumpis, "Modulation and Coding Techniques for the Space Shuttle Ku-Band TDRS Links," Axiomatix Report No. R7406-2 (Under NASA Contract NAS 9-13467), June 4, 1974.

22. B. D. Trumpis, "Computation of Probability of Error for Space Shuttle Convolutionally Encoded Links," Axiomatix Report No. R7407-2 (Under NASA Contract NAS 9-13467), July 10, 1974.

23. A. J. Viterbi, "Convolutional Codes and Their Performance in Communication Systems," IEEE Trans. Comm. Tech., October 1971.

24. B. D. Trumpis, "An Exhaustive Search for the Optimum Convolutional Code to be Used on the Space Shuttle Ku-Band Communication Link," Axiomatix Report No. R7407-3 (Under NASA Contract NAS 9-13467), July 11, 1974.

25. "Single Channel Monopulse Converters," Technical Bulletin No. D22873-1, Electromagnetic Sciences, Inc., Atlanta, Georgia.